

Rollerball-Pen-Drawing Technology for Extremely Foldable Paper-Based Electronics

Shuiren Liu, Junpeng Li, Xinlei Shi, Enlai Gao, Zhiping Xu, Honghao Tang, Kwing Tong, Qibing Pei, Jiajie Liang,* and Yongsheng Chen

It is reported that graphene oxide (GO) can work as the dispersing, associate thickening, stabilizing, adhesive, oxidation-resistant, and mechanical reinforcing agents simultaneously to formulate a drawable conductive ink with silver nanowire (AgNW). The synergistic effect of combining AgNW with GO can bring forth the AgNW-GO dynamic network, which imparts appropriate viscosity and rheological property to the ink for reliable rollerball-pen drawing on paper and plastic substrates and enables the drawn conductive traces to simultaneously possess high conductivity, remarkable foldability, and stability. The electrical conductivity of the rollerball-pen drawn electrodes with mild post-treatment condition by drying at 25 °C for ≈5 min after writing on paper can achieve 2.3×10^4 S cm⁻¹. The drawn electrodes are used as extremely foldable electrodes that can retain a record high conductivity of 1.4×10^4 S cm⁻¹ after 1000 folding–unfolding cycles. The feasibility of the drawable conductive ink is further demonstrated by fabricating paper-based conductive circuits and a capacitive touch screen sensor with outstanding foldability.

S. Liu, X. Shi, H. Tang, Prof. J. Liang, Prof. Y. Chen
 School of Materials Science and Engineering
 National Institute for Advanced Materials
 Nankai University
 Tianjin 300350, China
 E-mail: liang0909@nankai.edu.cn

Dr. J. Li
 School of Science
 Xi'an University of Technology
 Xi'an, Shaanxi 710048, China

E. Gao, Prof. Z. Xu
 Applied Mechanics Laboratory
 Department of Engineering Mechanics and Center for Nano and Micro Mechanics
 Tsinghua University
 Beijing 100084, China

K. Tong, Prof. Q. Pei
 Department of Materials Science and Engineering
 Henry Samueli School of Engineering and Applied Science
 University of California Los Angeles
 Los Angeles, CA 90095, USA

Prof. J. Liang, Prof. Y. Chen
 Key Laboratory of Functional Polymer Materials
 of Ministry of Education
 College of Chemistry
 Nankai University
 Tianjin 300350, China

DOI: 10.1002/aelm.201700098

1. Introduction

Foldable electronics, which can be folded, unfolded, and creased for storage in small spaces or formed into 3D self-standing structures, are considered as the essential components for the next-generation of electronics.^[1–6] Unlike flexible electronics which form a smooth curve on bendable or rollable substrates under relatively large bending radii (on the order of a few millimeters), foldable electronics generate extreme mechanical deformation with infinite radius and result in inelastic and permanent creases at the point of the folded line on the substrates or devices.^[1–3,7,8] Thus, developing truly foldable electronics entails the construction of foldable electronic components, such as conductors/electrodes, on foldable substrates that can withstand deformation while maintaining operational characteristics. Regarding substrate materials, ultrathin polymer films, such as polyethylene terephthalate (PET),^[9,10] polyimide,^[11] and parylene,^[12,13] with a thickness thinner than 10 μm have been successfully used as foldable substrates in foldable electronics. However, such free-standing ultrathin substrate inevitably suffers from mechanical instability of crumpling in some application fields.^[4] Paper is a micro or nanofiber-based texture material that is well known for its ability to be folded and unfolded to make many different types of 3D geometries.^[3] This ubiquitous property together with inexpensive, lightweight and disposable properties makes paper a promising alternative substrate for foldable electronics. Considering the features of paper, a major challenge to create paper-based foldable electronics is to develop a facile, cost-efficient, and compatible routine to construct foldable components, like conductor or electrodes, on paper substrate without using conventional high temperature or high vacuum processing conditions that are widely used in the semiconductor industry.

Various solution-based methods or technologies, i.e., direct-writing,^[5,14–16] transfer-printing,^[3,7,17] inkjet-printing,^[18–21] screen-printing,^[2,8,22,23] and so on, have thus been developed or employed on constructing devices on paper substrates.^[24,25] Of existing method of electrode construction, rollerball-pen-drawing technology, which uses the movement of a tiny ball as the writing point to transfer solvent-based liquid or gelled ink from a reservoir onto paper to draw patterns or traces, is the most unique approach used in paper-based electronics since

this technology can fully exploit the benefits of paper, including but not limited to it being portable, inexpensive, disposable, and printable/drawable.^[14–16] Generally, the characteristics of rollerball-pen drawn conductive electrodes are highly related to the properties and drawability of the conductive ink which depend on solid loading, particle dispersion, viscosity and rheology behavior, particle specific surface area and density, and so on. A number of publications and commercial products utilize metal-based micro or nanoscale fillers to formulate the conductive ink for rollerball pen.^[14–16] Lewis and co-workers reported a facile pen-on-paper approach for flexible paper-based electronics using rollerball pen filled with silver nanoparticles-based conductive ink.^[14] Recently, a bending device was also drawn on paper using copper nanowires-based ink in rollerball pen.^[15] Despite great success being achieved in the field of drawable paper-based electrodes, all these reported results or commercial products suffer either low electrical performance or limited foldability. So far, no one has succeeded in developing a rollerball-pen drawable ink with low cost, high conductivity, excellent mechanical compliance, long-term stability, and good adhesion with paper substrate for extremely foldable and printable paper-based electronics. Therefore, many important challenges still exist in developing high-quality drawable conductive inks for foldable and printable electronics.

Here we report the development of an ink that synergistically utilizes silver nanowires (AgNWs) and graphene oxide (GO) monolayer sheets for extremely foldable and drawable electronics. The work includes the following essential elements: (1) the conductive ink is prepared by formulating with small amount of AgNWs (≈ 4.7 wt% or ≈ 0.48 vol%) as conductive solid contents and GO monolayer sheets (≈ 0.59 wt% or ≈ 0.3 vol%) as the dispersing, associate thickening, stabilizing, adhesive, oxidation-resistant, and mechanical reinforcing agents simultaneously. (2) The efficient synergistic effect of silver nanowires and graphene oxide provides the inks with appropriate viscosity and rheological behavior reliable for rollerball-pen drawing on paper and plastic substrates. (3) The initial conductivity of the drawn electrodes with mild post-treatment of drying at 25 °C for around 5 min right after writing on paper can achieve as high as 2.3×10^4 S cm⁻¹ (average) and remain as high as 2.1×10^4 S cm⁻¹ after an accelerated stability test at 60 °C in air for 30 d. (4) The drawn electrodes on paper can be sharply folded repeatedly while retaining a high conductivity of $\approx 1.4 \times 10^4$ S cm⁻¹ after 1000 folding–unfolding cycles. (5) The excellent foldability of the drawn electrodes is enabled by the effective synergistic effects between AgNW and GO as supported by microscopy and bending-to-tension model analysis. (6) The ink allows the demonstration of extremely foldable and printable paper-based electronic circuits and projected capacitive touch screen sensor that are constructed by directly rollerball-pen drawing electrodes on paper substrates.

2. Results and Discussion

The key to the rollerball-pen-drawing technology is to identify a high performance conductive ink with the following features: (1) appropriate viscosity and shear thinning viscosity that stabilize the ink when stored in the pen barrel but can be lowered

when applying a shearing force caused by the rotation of the rollerball at high speed during the writing process when the ink is transferred onto the substrate; (2) drawn patterns/traces with good adhesion, high electrical performance, long-term stability, and mechanical compliance that can withstand extreme mechanical deformation. Generally, rollerball-pen-drawable conductive inks are composed of five essential components: conductive nano or microparticles, water or water-soluble organic solvent, a shear thinning viscosity property-providing agent, a lubricant, and a bubble suppressant. To develop an ink with the features as mentioned above, first, AgNWs with a length-to-diameter aspect ratio of as high as 500 instead of conventional metal nanoparticles or micro flakes were used as the conductive solid materials in present work to form percolation network with mechanical compliance and high electrical conductivity at low loading contents. However, the characteristic of high aspect ratio and high mass density could cause AgNWs to have a tendency to form entanglements and aggregations in the inks.^[15,18] To achieve uniform and stable AgNW inks, dispersing and stabilizing agents, like poly(vinyl pyrrolidone) (PVP), had to be added in the inks at relatives high loading density, which would thus inevitably decrease the conductivity of the final printed or drawn patterns. Moreover, the conductivity of AgNW networks tends to degrade gradually over time thanks to the oxidation issues commonly associated with nanoscale materials with large surface area.^[15,18] Thus, instead of using conventional polymer or organic-based additives in the ink formulation, GO monolayer sheet was chosen as associate thickening, dispersing, stabilizing, oxidation-resistant, and mechanical reinforcement agents simultaneously thanks to its multifunctional intrinsic properties and unique structure (as described in details below).^[26–28] Besides, FC4430, a nonionic polymeric fluorochemical surfactant which can contribute excellent wetting, spreading, and leveling properties to a variety of coating systems at very low concentration, was selected as a lubricant to prevent a ball and a tip seating surface from wearing and thus provide a smooth writing feeling and form uniform patterns on both paper and plastic substrates. In addition, distilled water was selected as solvent thanks to its environmental friendliness and low cost, and a tiny amount of PVP was added to further assist AgNWs in dispersing in water.

In a typical formulation, 2 mg mL⁻¹ GO dispersion was first made by dispersing GO monolayer sheets (average size ≈ 1 μm) in distilled water via sonication, followed by adjusting the pH value to 6.5 via adding 1 M NaHCO₃ aqueous solution. The GO dispersion was then added to the AgNW solution (1 wt% in distilled water) to induce rapid AgNW-GO coagulation which was collected by vacuum filtration using a polytetrafluoroethylene (PTFE) membrane filter with pore size of 0.45 μm to remove the undesired additives existing in the as-received raw AgNW solution. Next, a certain amount of distilled water, PVP, and FC4430 were added back to the AgNW-GO precipitate and redispersed the mixture through strong agitation to obtain the final homogeneous ink, named AgNW-GO-Ink. Careful optimization of the mass ratio between AgNW:GO:PVP:FC4430:water and 20:2.5:2:0.2:400 resulted in simultaneously best attributes of rheological properties, conductivity, stability, and mechanical compliance. For comparison, (hydroxypropyl)methyl cellulose (HPMC), a widely used water-soluble nonassociate thickening

agent, was used to replace GO to make inks (AgNW-HPMC-Ink) with the mass ratio between AgNW:HPMC:PVP:FC4430:water = 20:20:10:0.2:400. However, this solution was very inhomogeneous with a large amount of aggregations existing in the ink as shown from the photograph in Figure S1 (Supporting Information). Furthermore, another ink containing a high PVP content to achieve a homogenous AgNW ink without GO additive (named AgNW-PVP-Ink) was prepared. However, to achieve uniform dispersion of drawable AgNW ink, the PVP content has to be increased substantially (AgNW:PVP:FC4430:water = 20:20:0.2:400), which leads to a relatively lower conductivity of the final drawn patterns. Besides, two commercial drawable conductive pens were also obtained for comparison in the

present work: one containing silver nanoparticles as the conductive solids (AgNP-Ink, Circuit Scribe, Electrominks Incorporated) and the other one employing silver microflakes as the conductive additives (AgMF-Ink, CW2200, CircuitWorks).

The viscosity and rheological behavior of the drawable inks, which significantly affect the pen-on-paper drawing process and the final drawn electrode performance, was first investigated using a cone-plate rheometer. **Figure 1a** exhibits the measured viscosity at different shear rates from the steady-state flow step test for pure GO aqueous suspension (GO:water = 2.5:400) with GO concentration of ≈ 0.3 vol% and GO-PVP-FC4430 aqueous solution (GO:PVP:FC4430:water = 2.5:2.0:0.2:400). It clearly shows that the viscosity of both solutions without

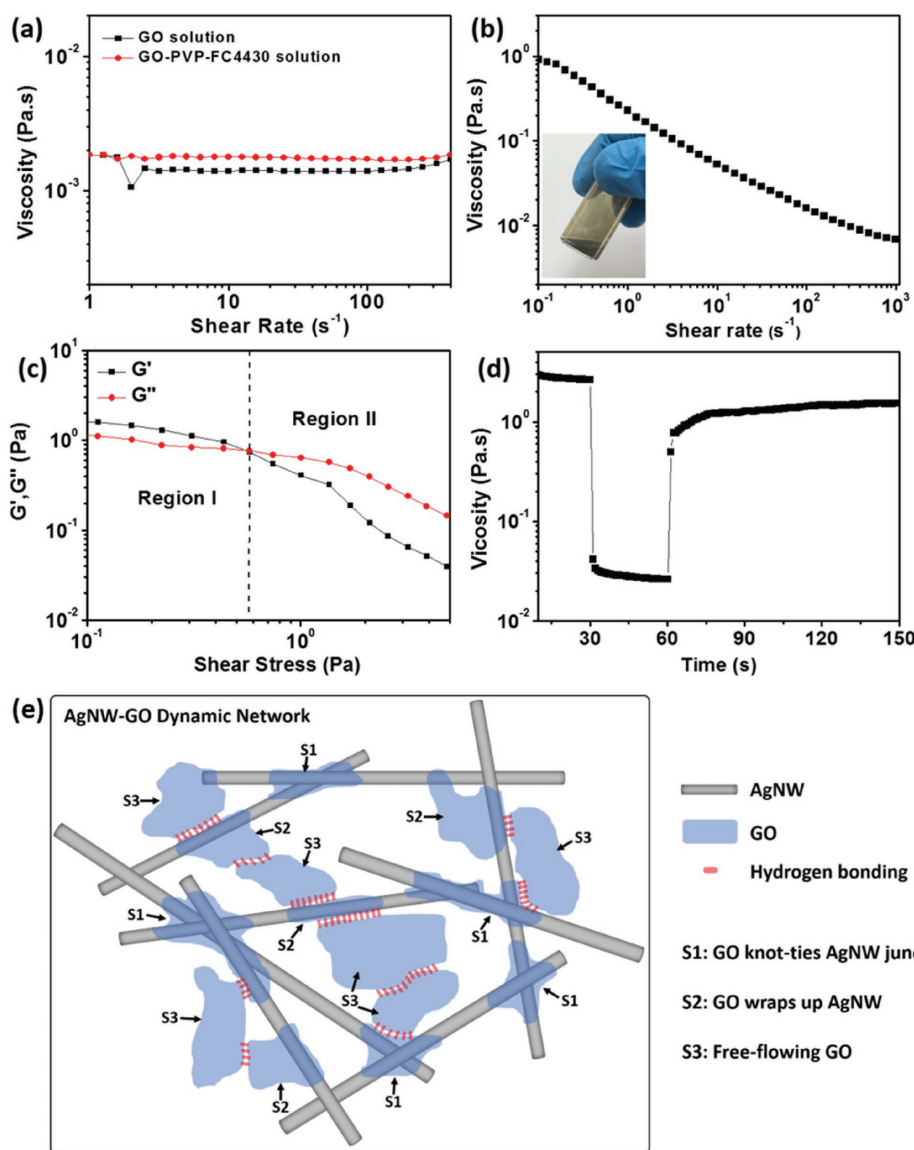


Figure 1. Viscosity as a function of shear rate for a) GO and GO-PVP-FC4430 solution and b) AgNW-GO-Ink. The inset shows the photograph of the as-prepared AgNW-GO-Ink. c) Variation of G' and G'' with shear stress for AgNW-GO-Ink. d) Rheological behavior of the AgNW-GO-Ink during simulation of rollerball-pen drawing. e) Schematic illustration of associative thickening of AgNW-GO-Ink via dynamic AgNW-GO network. GO is present in the inks as three states: S1, GO knot-ties and solders the AgNW junctions; S2, GO warps up the AgNWs; S3, GO free flows in the ink. The cohesion of the AgNW-GO dynamic network stems from the hydrogen bonding.

adding AgNWs is almost the same and is constant at different shear rates, indicating a Newtonian behavior. Shear thinning thixotropic behavior and unique viscoelastic properties were widely observed and investigated for concentrated GO aqueous dispersion.^[29,30] The Newtonian behavior observed for both GO and GO-PVP-FC4430 aqueous solution in present work suggests that the GO concentration of ≈ 0.3 vol% in the dispersion is not high enough to lead the GO monolayer sheets to interconnect to form a reversible and dynamic network. However, the AgNW-GO-Ink with the addition of ≈ 0.48 vol% (≈ 4.7 wt%) of AgNWs possesses much improved viscosity value (> 1 Pa s at a shear rate of 0.1 s $^{-1}$) and displayed shear thinning thixotropic behavior as shown in Figure 1b. The most likely scenario is that AgNWs and GO monolayer sheets form a reversible and dynamic network in the ink which leads to associative thickening effect. This network and thickening effect are schemed in Figure 1e. According to the theoretical prediction of percolating rod network system, the concentration of 0.48 vol% for AgNW with an aspect ratio of ≈ 500 is much higher than its percolation value,^[31,32] indicating AgNWs can form a continuous network in the ink if the AgNWs are homogeneously dispersed in the solution. However, only AgNWs in the solution cannot generate rheological behavior since (1) the interactions or junctions between AgNWs are very weak, and (2) only AgNWs without any dispersing agents are not able to form a uniform dispersion. Thus, the incorporation of GO in the ink is critical to ensure the rheological behavior. In fact, although the concentration of GO (≈ 0.3 vol%) in the dispersion is not high enough to generate rheological behavior, the unique amphiphilic structure of GO, which contains both hydrophilic regions contributed by the oxygen-containing function groups and hydrophobic regions made by the unoxidized polyaromatic graphene islands,^[33] makes this soft 2D material to be capable of acting as associate thickeners. As illustrated in Figure 1e, GO is present in the AgNW-GO-Ink mainly as three states. GO not only can assist AgNWs to disperse well to form a continuous network in the ink but also is able to enhance the strength of AgNWs junctions or linkage points through wrapping around and soldering the junctions without sacrificing their flexibility (State 1, S1).^[34] Moreover, the GO monolayer sheets that adhere on or wrap around AgNWs (State 2, S2) can further improve the cohesion and interaction between AgNW-GO network and individual free-flowing GO (State 3, S3) and water molecular through hydrogen bonding. Thus, the enhanced strength of the AgNW-GO dynamic networks and the strong interaction between the AgNW-GO networks and surrounding solvent and additives ensure the efficient associate thickening behavior for the AgNW-GO-Ink (Figure 1e).

Oscillatory rheological measurements were further carried out for AgNW-GO-Ink using a stress sweep step (SSS) test and the elastic G' (storage modulus) and viscous G'' (loss modulus) as a function of shear stress for the ink are displayed in Figure 1c. The curves can be divided into two regions.^[35–37] In Region I, the storage and loss moduli for AgNW-GO-Ink are completely and clearly well-separated from each other at the shear stress lower than 0.58 Pa, which indicates that the AgNWs and GO in the ink can form tenuous network architecture with an elastic-dominant part in spite of the relatively low concentration of each additive. However, the elastic G' and

viscous G'' both declined gradually with increasing shear stress, while the value of G' remained higher than G'' . This indicates the beginning of the weakening of the AgNW-GO junctions and linkages and thus the gradual breakdown of the AgNW-GO network structure in the ink. Although the AgNW-GO-Ink still has an elastic-dominated behavior ($G' > G''$) in Region I, it exhibits a more liquid-like behavior as shear stress increased.^[37] After the $G'-G''$ crossover point (at a shear stress of 0.58 Pa), Region II starts and the G'' becomes higher than G' with increasing shear stress, indicating a liquid-dominant behavior for the AgNW-GO-Ink.^[38,39]

Next, the rheological properties of the AgNW-GO-Ink during rollerball-pen drawing was investigated via a peak hold step (PHS) test consisting of holding the sample at different shear rates in three intervals, as shown in Figure 1d. The shear rate remained at 0.1 s $^{-1}$ for 30 s in the first interval, then increased to 100 s $^{-1}$ and held for 30 s in the second interval to simulate the rotation the tip ball, and finally decreased to 0.1 s $^{-1}$ and held for an additional 100 s in the third interval to explore the viscosity recovery after drawing. The viscosity of the AgNW-GO-Ink decreased from ≈ 3 Pa s at 0.1 s $^{-1}$ to ≈ 0.03 Pa s after shearing at 100 s $^{-1}$ at time of 40 s. Then, the viscosity recovered very quickly to ≈ 1.3 Pa s only in 30 s (at the time of 90 s) after reducing the shear rate in the third interval. This appropriate viscosity together with excellent rheological behavior renders the AgNW-GO-Ink very reliable for rollerball-pen drawing. A suitable viscosity of 1–3 Pa s can stabilize the AgNW-GO-Ink in the ink barrel without leaking from the ballpoint tip when no shearing force was applied. When a shearing force caused by a ball rotating during the drawing process was applied, the ink in the vicinity of the ball would have lower viscosity and the loss modulus would become dominant (thinning effect), allowing the uniform AgNW-GO-Ink transfer onto a paper substrate without skipping and clogging. When the ink leaves the ball tip and sit on the substrates, the entanglement and bridging of GO and AgNWs reform the AgNW-GO network and thus lead the AgNW-GO-Ink to regain high elasticity and retain the drawn structures or patterns, making it possible to draw fine lines with smooth edges and appropriate thickness to offer low sheet resistance.

Next, we investigated the electrical properties of the AgNW-GO-Ink electrodes drawn on paper substrates via rollerball-pen-drawing technique. The inset photograph in Figure 2a presents the image of three AgNW-GO-Ink traces on paper drawn by rollerball pen with three typical tip ball diameters of 550, 800, and 960 μm , respectively. The line width of the continuous and uniform trace drawn by rollerball pen with a ball diameter of 960 μm is around 900 μm as shown in Figure S2 (Supporting Information). Unless otherwise stated, all AgNW-GO-Ink electrodes or circuits drawn on paper substrates in the present work were using rollerball pen with a tip ball diameter of 960 μm . The drawn AgNW-GO-Ink electrode exhibits a continuous and dense network/mesh structure without obvious bundles or aggregations of AgNWs (Figure 2a), another indication of uniform dispersion of AgNWs in the ink. Furthermore, it is important to note that uniform and smooth AgNW-GO-Ink traces can also be drawn on a polymer substrate, such as PET (Figure S2, Supporting Information), thanks to the addition of surfactant and wettability agent FC4430. This indicates that

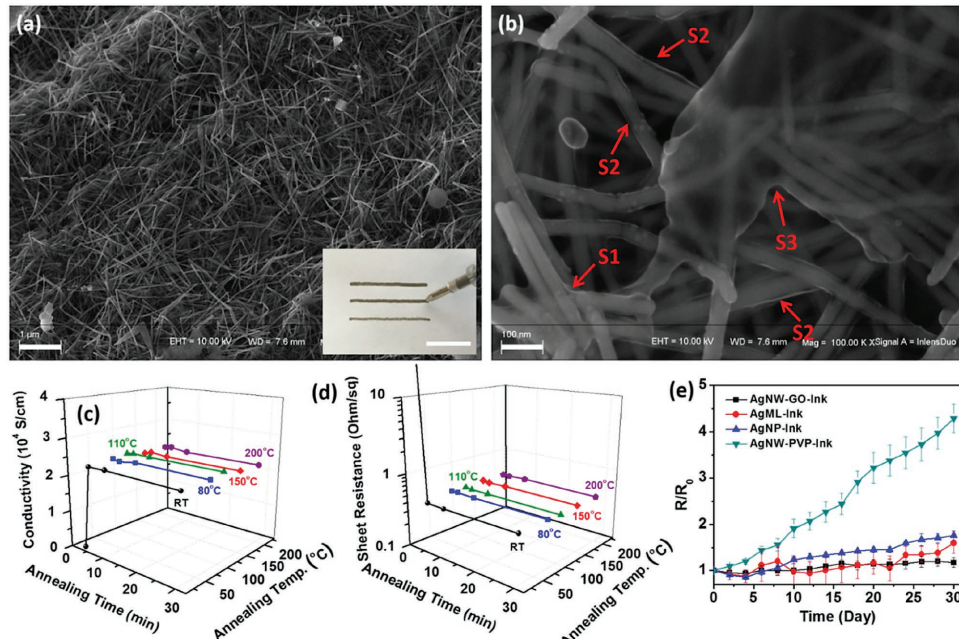


Figure 2. a) SEM image of the top view of an AgNW-GO-Ink electrode drawn on paper, and scale bar is $1\text{ }\mu\text{m}$. The inset shows the photograph of AgNW-GO-Ink electrodes with different width drawn on a paper by rollerball pen with different ball diameters. Scale bar is 1 cm . b) Magnified SEM image of AgNW-GO-Ink electrode showing three states of GO existing in the electrode (indicated by red arrows): S1, GO knot-ties AgNW junctions; S2, GO wraps around AgNWs; S3, free-flowing GO lies on top of the electrode. Scale bar is 100 nm . c) Electrical conductivity and d) sheet resistance of AgNW-GO-Ink electrodes as a function of drying temperature and time. e) Plots of relative resistance change versus time for AgNW-GO-Ink, AgNW-PVP-Ink, AgNP-Ink, and AgMF-Ink electrodes drawn on paper substrates after exposure to hot air at $60\text{ }^\circ\text{C}$ for 30 d . More than five samples for each electrode were measured for the electrical conductivity and stability tests.

AgNW-GO-Ink is able to be employed to directly construct or repair electrical circuits using rollerball-pen-drawing technique on practical plastic circuit boards. Interestingly, from the magnified SEM image in Figure 2b for the drawn AgNW-GO-Ink electrode, it can be clearly seen that there are three states of GO existing in the drawn electrode. In S1, GO monolayer sheets warp around and knot-tie the AgNW junctions acting as soldering material. In S2, working as a barrier film, GO monolayer sheets warp up and pack the AgNWs. In S3, GO monolayer sheets lie on top of the electrode acting like free-flowing sheets without warping any AgNW. In fact, the observed three states of GO in the electrode are also consistent with the AgNW-GO dynamic network structure in the AgNW-GO-Ink as illustrated in Figure 1e.

Significantly, the AgNW-GO-Ink electrodes became conductive with post-treatment of drying at room temperature of about $25\text{ }^\circ\text{C}$ for only 3–4 min right after drawn on paper, exhibiting an electrical conductivity of $\approx 10\text{--}25\text{ S cm}^{-1}$ and a sheet resistance of $\approx 200\text{--}500\text{ }\Omega \text{ sq}^{-1}$. Upon drying for around 5 min at $25\text{ }^\circ\text{C}$, a significant increase in the conductivity was observed, and an average electrical conductivity of $\approx 2.3 \times 10^4\text{ S cm}^{-1}$ and an average sheet resistance of $\approx 0.44\text{ }\Omega \text{ sq}^{-1}$ were achieved for the AgNW-GO-Ink electrodes drawn on a paper substrate (Figure S3 and Movie S1, Supporting Information). If drying the AgNW-GO-Ink electrodes at $110\text{ }^\circ\text{C}$ right after writing on papers, only less than 2 min of drying time was required to achieve the best electrical conductivity. Interestingly, prolonged drying time (up to 30 min) and increased drying temperature

(up to $200\text{ }^\circ\text{C}$) do not considerably increase the electrical conductivity of the AgNW-GO-ink electrodes as shown in Figure 2c (Figure S4, Supporting Information) and Figure 2d (Figure S5, Supporting Information). Such high conductivity for the AgNW-GO-ink electrodes achieved under such mild post-treatment conditions is mainly ascribed to the effective synergistic effects between AgNW and GO. First, during the drying process, the intrinsic excellent flexibility and high toughness properties for GO make GO monolayer sheets act as soldering material to wrap around and knot-tie the AgNW junctions (S1 of GO) due to the electrostatic force as well as capillary force (Figure 2b).^[34] The great reductions for inter-nanowire contact resistance in the AgNW network can thus be achieved through the tightly knot-tied AgNW junctions by GO without conventional high-temperature thermal sintering process.^[34] Second, the effective multifunction characteristics of GO, simultaneously working as associate thickening, dispersing, stabilizing, protecting, and mechanical reinforcement agents in the AgNW-GO-Ink, can largely reduce the loading contents of the electrical insulating additives in the final electrodes. In comparison, conventional conductive inks consisting of metal conductive particles and polymer-based additives requires higher annealing/curing temperature and longer post-treatment time to thermally fuse the metal particles or decompose the excess insulating additives.^[14,16] **Table 1** compares the electrical performance of rollerball-pen drawn AgNW-GO-Ink electrodes with a number of previously published results and commercial products concerning directly pen-drawable or writable conductive inks based

Table 1. Comparison of electrical conductivity of the present work with various previous research and commercial products concerning drawable inks.

Solid contents	Drawing method	Post-treatment conditions	Electrical conductivity [S cm^{-1}]	Drawn line resistance [$\Omega \text{ cm}^{-1}$]	Ref.
Silver nanoparticle 50 wt%	Rollerball pen drawing	25 °C, 30 min	$\approx 5.00 \times 10^3$	≈ 12	[14]
Silver nanoparticle 50 wt%	Rollerball pen drawing	200 °C, 30 min	$\approx 2.50 \times 10^5$		[14]
Silver nanoparticle	Rollerball pen drawing	25 °C, 2 min		2–10	Circuit Scribe, Electroninks Incorporated
Silver nanoparticle 20 wt%	Rollerball pen drawing	200 °C, 60 min	$\approx 1.47 \times 10^5$	$\approx 11.8\text{--}12.2$	[16]
Silver microflake	Valved pen tip drawing	150 °C, 5 min	$\approx 2 \times 10^4$		CW2200, Circuit Works
AgNW 5 wt%	Needle tip direct writing	Flashlight sintering		$\approx 100\text{--}1000$	[5]
AgNW 5 wt%	Needle tip direct writing	25 °C, 24 h		Few kΩ ranges	[5]
Copper nanowires 18.28 wt%	Rollerball pen drawing			$\approx 100\text{--}1000$	[15]
AgNW-PVP-Ink, 4.5 wt%	Rollerball pen drawing ^{a)}	110 °C, 5 min	4.6×10^3	$\approx 10\text{--}20$	Present work
AgNW-GO-Ink, 4.7 wt%	Rollerball pen drawing ^{a)}	25 °C, 5 min	2.3×10^4	$\approx 2\text{--}4$	Present work

^{a)}Ball diameter is 960 μm.

on metal nanoparticles/microflakes/nanowires. It clearly shows that AgNW-GO-Ink electrodes in present work exhibit one of the best conductivity under mild post-treatment conditions (25 °C or low temperature drying at short time), and the electrical performance is much better than other reported metal nanowires-based inks.^[5,15] Although conductive inks based on silver nanoparticles and microflakes displayed better electrical performance when sintering or annealing at high temperature (≈ 200 °C) with longer post-treatment time (>30 min),^[14,16] such harsh post-treatment conditions are not compatible with the paper-based electronic applications.^[5]

Long-term storage stability is another important requirement for paper-based electronics. Figure 2e presents the resistance change versus time for AgNW-GO-Ink, AgNW-PVP-Ink, AgNP-Ink, and AgMF-Ink electrodes drawn on paper substrates during the accelerated test at 60 °C in air over 30 d. The resistance of AgNP-Ink and AgMF-Ink electrodes has a tendency of slight increase over testing time and reaches to 1.8 and 1.6 times their initial values. However, the resistance for AgNW-PVP-Ink electrode exhibits a much greater increase and rises to 4.3 times its initial values after 30 d. The resistance increase is mainly attributed to surface oxidation issue of the nanoscale or microscale silver fillers caused by the attack from environmental oxygen and sulfur.^[40,41] In contrast, the resistance of the AgNW-GO-Ink electrode increased by a mere $\approx 15\%$ after 30 d. It is suggested that the GO wrapping around the AgNWs and their junctions (Figure 2b) can work as a barrier layer (S1 and S2 of GO) to impede the AgNWs from reacting with environmental oxygen and sulfur.^[34,40,41]

We further investigated the mechanical folding stability of the AgNW-GO-Ink electrode drawn on paper substrates. It should be mentioned that different from bending substrates or devices, inelastic and permanent creases at the point of folded line on substrates or devices will appear when folding electronics (Figure 3a and Figure 4), indicating larger tensile strain applied on the folded substrates and devices. To test the foldability of the electrodes, conductive lines with dimensions of 20 mm in length and $\approx 700\text{--}900$ μm in width were drawn on paper substrates, and the testing samples were folded and compressed by hand at the folded edge until the surfaces of

the papers were firmly pressed against itself to guarantee a smallest achievable bending radius by folding. Figure 3b and Figure S6 (Supporting Information) display the normalized resistance (R/R_0 , the ratio of instantaneous resistance under folded state to the initial resistance without folding) for AgNW-GO-Ink, AgNW-PVP-Ink, AgNP-Ink, and AgMF-Ink electrodes drawn on paper substrates during 1000 repeated folding-unfolding cycles. More than eight samples of each electrode were measured, and the variation of resistance change among the samples in each group was within $\pm 20\%$. The AgNW-PVP-Ink, AgNP-Ink, and AgMF-Ink electrodes show 2.5-fold, 2.7-fold, and 3.9-fold increase in resistance after one folding-unfolding cycle, respectively. The resistance of AgNW-PVP-Ink electrodes gradually increased to about 73 times its initial value after 1000 cycles, and the resistance for both AgNP-Ink and AgMF-Ink electrodes displayed a sharp increase in the following cycles with the electrodes becoming nonconductive after 100 and 30 folding-unfolding cycles for AgNP-Ink and AgMF-Ink, respectively. In contrast, the resistance of AgNW-GO-Ink electrode remained fairly stable during the testing of 1000 folding-unfolding cycles with a slight increase in its resistance of only 1.7 relative to its initial and unfolded value (corresponding to a record high conductivity of $\approx 1.4 \times 10^4$ S cm $^{-1}$). Next, we further compared the foldability of different conductive inks on paper substrates by connecting LED chips with conductive circuits respective made of AgNW-GO-Ink, AgNP-Ink, and AgMF-Ink on papers as shown in Figure 3c. It can be observed that the LED chip still operated well on the AgNW-GO-Ink circuit on paper after 30 cycles of folding-unfolding (Movie S2, Supporting Information); however, the LED chips on both AgNP-Ink and AgMF-Ink circuit on paper were non-functional after 30 cycles of folding-unfolding. Moreover, we also demonstrated that LED chip on conductive circuits drawn by AgNW-GO-Ink on paper could work very well before crumpling (Figure 3d), under complicated crumpling (Figure 3e), and after uncrumpling (Figure 3f).

To understand the mechanism of outstanding foldability of the AgNW-GO-Ink electrodes drawn on papers, a more thorough study of the crack formation of the electrodes after folding and unfolding cycles was investigated. Figure 4a-d

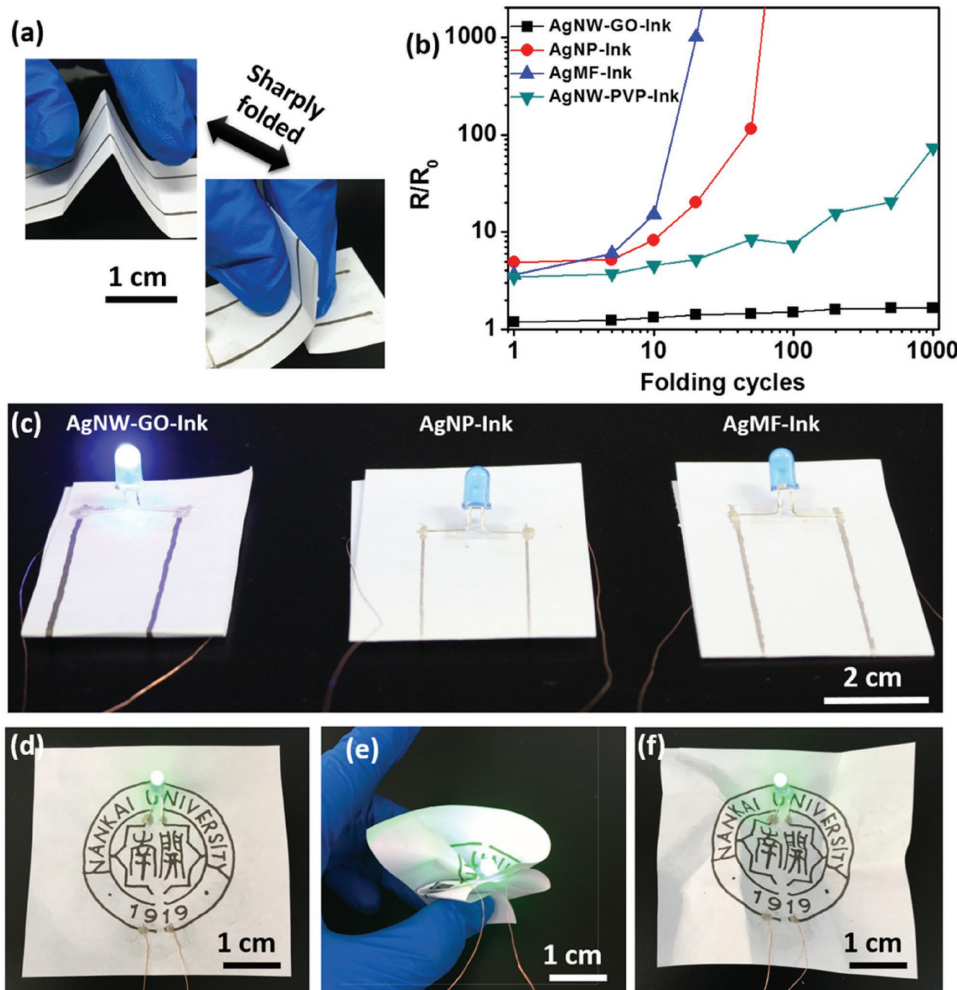


Figure 3. a) Photographs of AgNW-GO-Ink electrodes drawn on a paper substrate while being sharply folded with permanent mechanical deformation at the point of folded line. b) Relative resistance change of AgNW-GO-Ink, AgNW-PVP-Ink, AgNP-Ink, and AgMF-Ink electrodes drawn on paper substrates during 1000 repeated folding-unfolding cycles. c) Photographs of operation of LED chips with AgNW-GO-Ink, AgNP-Ink, and AgMF-Ink circuits drawn on paper substrates under sharply folded state after 30 folding-unfolding cycles. Operation of an LED chip on conductive circuits drawn by AgNW-GO-Ink filled rollerball pen on a paper substrate d) before, e) during, and f) after crumpling.

shows SEM images of AgNW-GO-Ink, AgNW-PVP-Ink, AgNP-Ink, and AgMF-Ink electrodes drawn on paper substrates after one folding-unfolding cycle. A big crease at the point of folded line on the electrode-patterned substrate is clearly observed on all four folded samples. Since the electrodes are on top of the substrates, the formation of the crease on the substrates caused by tensile stress when folding indicates that the drawn electrodes are stretched at the point of fold.^[3] The tensile stress generated large fractures and cracks on AgNW-PVP-Ink, AgNP-Ink, and AgMF-Ink electrodes. Some parts of the AgNW-PVP-Ink and AgNP-Ink electrodes are obviously delaminated from the creases of the paper substrates, and parts of AgMF-Ink electrodes are even peeled off from the substrate. These large fractures and cracks are mechanical defects of the electrode that can drastically affect the conductivity of the electrodes and circuits as shown in Figure 3b. After 30 folding-unfolding cycles, although some parts were still connected, a large portion of the

AgNP-Ink electrode was peeled off the substrate (Figure 4g), inducing a severe increase in the resistance (> 100-fold increase as shown in Figure 3b); moreover, a complete breakage along the width of the AgMF-Ink electrode on the crease was clearly seen in Figure 4h, which thus caused a complete loss of the conductivity of the electrodes, consistent with the results presented in Figure 3b. This poor foldability for the AgNP-Ink and AgMF-Ink electrodes on paper substrates is mainly due to (1) the relatively rigid structure of the conductive electrodes composed of nanoparticles (Figure 4k) and microflakes (Figure 4l) with low aspect ratio and (2) the relative poor adhesion between the electrodes and cellulose fiber-based paper. As to the AgNW-PVP-Ink electrodes on paper, although a number of large fractures, cracks, and even electrode delamination appeared on the electrodes after one folding-unfolding cycle, these breaks remained relatively intact and did not propagate into larger defects in the subsequent 1000 folding-unfolding cycles. It is suggested that the sliding of AgNWs in the AgNW-PVP-Ink

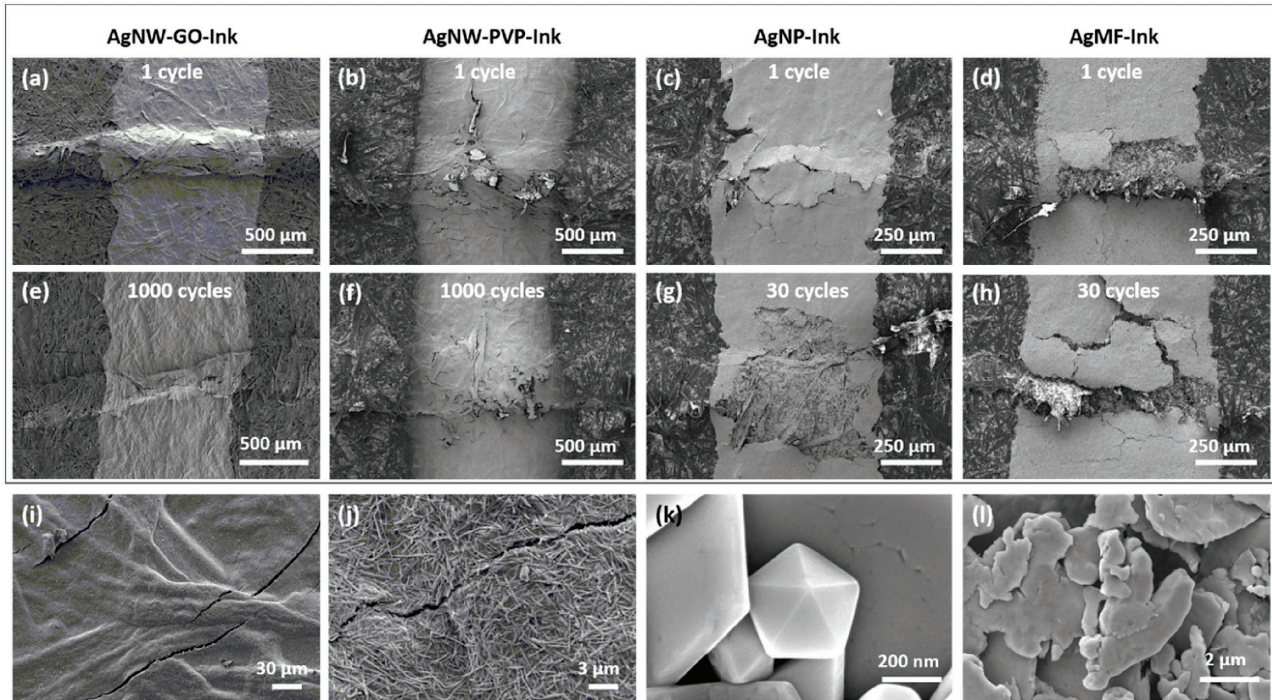


Figure 4. SEM images of a) AgNW-GO-Ink electrode, b) AgNW-PVP-Ink electrode, c) AgNP-Ink electrode, and d) AgMF-Ink electrode drawn on paper substrates after one cycle of folding–unfolding with permanent creases at the point of folded line on paper substrates. SEM images of e) AgNW-GO-Ink electrode and f) AgNW-PVP-Ink electrode drawn on paper substrates after 1000 cycles of folding–unfolding. SEM images of g) AgNP-Ink electrode and h) AgMF-Ink electrode drawn on paper substrates after 30 cycles of folding–unfolding. SEM images of i) microscale cracks and j) nanoscale cracks appearing on the AgNW-GO-Ink electrode drawn on a paper substrate after one cycle of folding–unfolding. SEM images of k) silver nanoparticles in the AgNP-Ink and l) silver microflakes in the AgMF-Ink.

conductive network can accommodate a part of strain applied to the electrodes, resulting in better flexibility than the conductive network made of nanoparticles or flakes.^[7] Interestingly, the AgNW-GO-Ink electrode drawn on paper showed much different surface morphology after being subjected to folding–unfolding cycles. As can be seen from the SEM image in Figure 4a, a very uniform film wrapping around the crease without any electrode delamination or peel-off was observed for AgNW-GO-Ink electrode after one folding cycle. Fractures with microscale crack width (<1.5 μm) aligned parallel to the folding line were observable in the folded AgNW-GO-Ink electrode (Figure 4i); besides, nanoscale fractures with a crack width smaller than 200 nm were also formed on the folded AgNW-GO-Ink electrode (Figure 4j). The size and quantities of these micro and nanofractures on the AgNW-GO-Ink electrode maintained fairly stable in the following 1000 folding–unfolding cycles (Figure 4e) and thus only introduced a very slight decline to the conductivity of the electrode (Figure 3b). It is believed that the remarkable foldability of AgNW-GO-Ink electrodes is mainly attributed to the following three reasons. First, the GO sheets that wrap around and solder the AgNW junctions can greatly improve the mechanical strength of the conductive network junctions or linkages, which can accommodate a large portion of applied strain as discussed below (Figure 5). Second, the formation of micro and nanofractures during folding could also accommodate a portion of applied strain without greatly decreasing the conductivity. It can be seen that despite the appearance of the nanoscale cracks, a large portion

of the AgNWs still remained connected (Figure 4j); moreover, compared to the width of the drawn electrode, the length of the micro and nanoscale fractures is approximately an order of magnitude smaller and thus would not result in much decrease in conductivity. Third, the oxygen-containing function groups on GO can lead to favorable adhesion between the AgNW-GO-Ink electrodes and the cellulose-based paper surface via hydrogen bonding. This good adhesion could contribute the ability of AgNW-GO-Ink to withstand delamination and peel-off from the paper substrate.^[3] It can be seen from Figure S7 (Supporting Information) that the AgNW-GO-Ink electrodes even have good adhesion with PET substrate. 100 repeated adhesion-peeling cycles with 3M Scotch adhesive tape does not alter the resistance of AgNW-GO-Ink electrodes drawn on PET substrate.

A mechanical model from folding to tension is used to further analyze the excellent foldability of AgNW-GO-Ink electrode on paper. The folding of AgNW-GO-Ink electrode on paper can be treated as a beam model under extremely bending deformation, as shown in Figure 5a. The curvature can be expressed as

$$1/\rho = 2\epsilon_g/h \quad (1)$$

where $2\epsilon_g$ is strain gradient (one side of the beam is under tensile strain ϵ_g and the other side is under compressive strain $-\epsilon_g$), h and ρ are the thickness and curvature radius of the beam, respectively. As measured in the experiments, the thickness of paper h_1 and drawn electrode h_2 is about 88 and

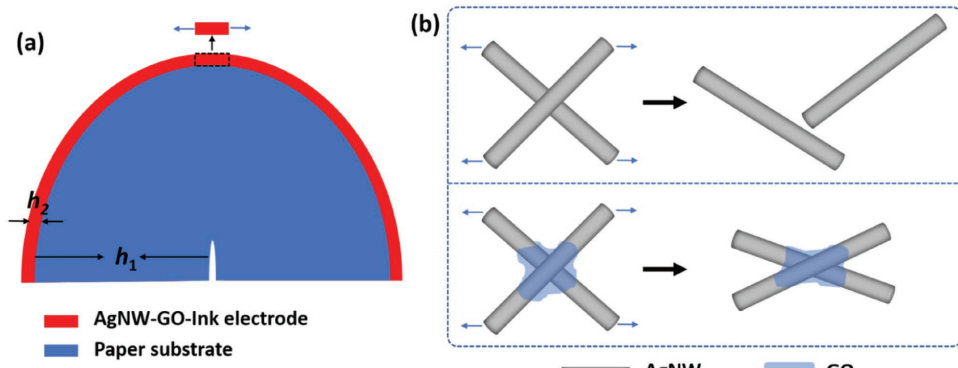


Figure 5. a) The mechanical model from folding to tension. b) Deformation mechanism of the conductive network without and with GO.

1 μm , respectively. Accordingly, the strain of AgNW-GO-Ink electrode can be calculated from $0.98\varepsilon_g$ in the interface to $1.00\varepsilon_g$ of the outer surface, and the AgNW-GO-Ink electrode thus can be approximately seen under a tensile strain $1.00\varepsilon_g$. Moreover, the first-principles calculation shows that the surface energy of silver (AgNW/AgNW) and graphene on silver (G/AgNW) are $\approx 0.72 \text{ J m}^{-2}$ ^[42] and $\approx 0.46 \text{ J m}^{-2}$ ^[43] respectively. The diameter and length of AgNW are $\approx 35 \text{ nm}$ and $\approx 20 \mu\text{m}$, and the thickness and lateral size of GO are $\approx 1 \text{ nm}$ and $\approx 1 \mu\text{m}$, respectively. Hence, the junction energy of AgNW/AgNW and G/AgNW in AgNW-GO-Ink electrode was estimated to the order of $\approx 10^{-16} \text{ J}$ and $\approx 10^{-14} \text{ J}$, respectively. Then, a mechanism as sketched in Figure 5b is proposed. When GO is incorporated into the AgNW network, junctions or linkages of GO wrapping AgNWs are formed, which is hundreds of times stronger than that of AgNW/AgNW junctions, and thus the AgNW-GO network can bear larger strain than that without GO. Furthermore, hinging the joints by flexible yet very tough GO monolayer sheets can allow the twist of G/AgNW junctions without significant sliding and disjointing when folding.

To demonstrate the application potential of the drawable AgNW-GO-Ink in foldable paper-based electronics, an entire capacitive and foldable touch sensor and the corresponding touch screen system were developed and evaluated. As shown in Figure 6a, row electrodes and column electrodes, both made of eight alternating active electrodes and a shared ground electrode, were respectively drawn on the top side and bottom side of one paper substrate with a stacked angle of 90° by rollerball-pen drawing with AgNW-GO-Ink. An active electrode couples with a neighboring ground electrode to form a capacitor, and thus a paper-based capacitive touch sensor with touch sensing circuitry of 8×8 independently controlled sensor pixels was constructed (Figure S4, Supporting Information). It should be noted that all the electrode patterns with different line width were drawn directly by rollerball pen with different ball diameter without using any mask or stencil. Figure 6b demonstrates the working principle of the capacitive touch sensor. Briefly, the capacitance between one active electrode and ground electrode under the untouched state (C_u) is equal the intrinsic capacity value (C_0) of the capacitor, which is mainly dependent on the resistance, line width and line spacing of the electrodes and the surrounding environment. When a finger touches the sensor, the electric field between the electrodes is modified

and the capacitance (C_t) is increased to C_0 associated with the finger capacitance (C_f). Figure 6c illustrated a sensing point of the capacitive touch sensor being formed at an overlap of coupling row and column electrodes, and the touch location can be determined via the capacitance changes on both a row electrode and a column electrode when touched by a finger. It should be pointed out that no circuit shorting phenomenon caused by ink permeation from overlap electrodes drawn on both sides of the paper was observed thanks to the large length of AgNWs that prevents the conductive fillers from passing through the fiber-based paper (Figure S8, Supporting Information). This suggests the possibility of making ultrathin paper-based electronics on both sides of one piece of paper using our AgNW-GO-Ink as electrodes and paper substrate as an insulating or dielectric layer.

The paper-based capacitive touch sensor with an array of 8×8 capacitive touch sensing points was then connected to an 8×8 light-emitting diode (LED) display through an Arduino microcontroller to construct an entire capacitive touch screen system (Figure 6d).^[44] Arduino is able to apply 5 V as a step input to a resistor and a capacitor in series and measure the time required for the potential on the capacitor to reach 2 V,^[45] as detailed in supporting information (Figure S9, Supporting Information). In brief, when a finger touches, the sensor capacitance increases from C_u to C_t , and the charging time of an input potential also increases. The touch screen system can detect the additional charging time of the electrodes in the finger-touching state relative to a fixed threshold. If both charging times of a row electrode and a column electrode are detectable, a sensing point is located and the corresponding LED pixel is turned on. The optical photos in Figure 6d and Movie S3 (Supporting Information) demonstrate the touching function of the capacitive touch screen system through showing a figure "8" on the LED display by a fingertip drawing on the paper-based capacitive touch sensor. The foldability of the paper-based capacitive touch sensor is then further demonstrated in Figure 6e and Movie S3 (Supporting Information). As can be seen, the entire figure "8" could be drawn on the LED display again after the paper-based capacitive touch sensor is multifolded and unfolded, revealing good foldability of the AgNW-GO-Ink electrodes drawn on paper substrates. Thus, this rollerball-pen-drawing technology based on our AgNW-GO-Ink provides a facile yet versatile routine to fabricate foldable, printable, and portable electronics for practical next-generation electronic applications.

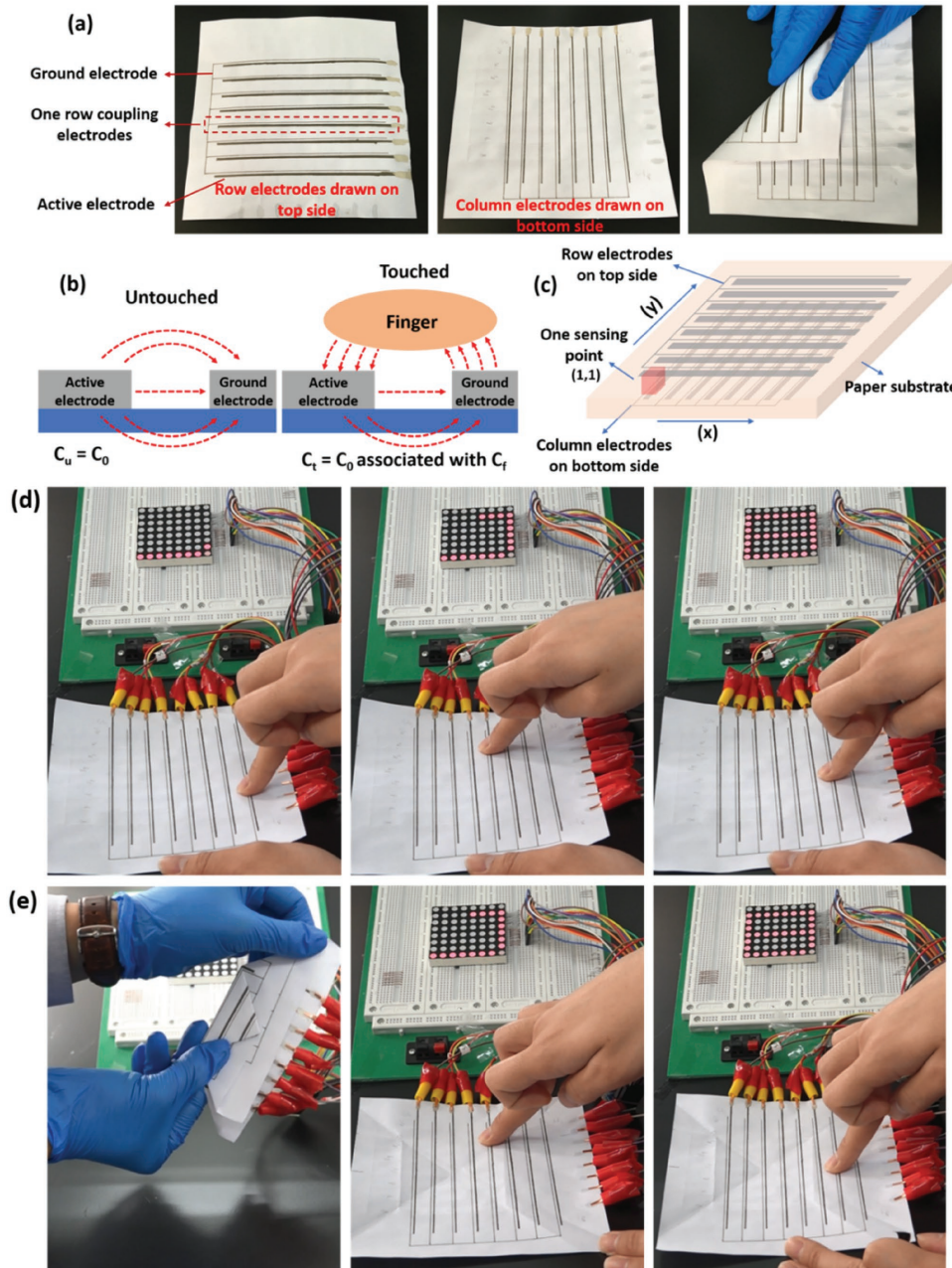


Figure 6. a) Optical photographs of paper-based touch sensor fabricated by drawing AgNW-GO-Ink-based row electrodes on the top side and column electrodes on the bottom side of a paper substrate with a stacked angle of 90°. b) The electric field and capacitance change when a finger approaching the coupling electrodes. C_u and C_t represent the capacitance of touch sensor under untouched and touched states respectively; C_0 and C_f represent the intrinsic capacitance value of the untouched touch sensor and finger capacitance. c) Schematic of row electrodes and column electrodes stacked at 90° angle on the top side and bottom side of a paper substrate respectively with a located sensing point. d) A capacitive touch screen system shows that a figure "8" was drawn on an 8 × 8 LED display controlled by the paper-based touch sensor. e) Demonstration of the foldability of the paper-based touch sensor. The entire figure "8" can be drawn again on the display after the paper touch sensor was multifolded and unfolded.

3. Conclusion

In summary, a new type of water-based rollerball-pen ink with AgNWs as the conductive solid contents and GO monolayer sheets as the multifunctional additives was developed. The effective synergistic effects between AgNWs and GO introduce a number of unique and excellent features for the conductive

inks and the drawn electrodes. Suitable viscosity, rheological behavior, and wettability of the AgNW-GO-Ink render it very reliable for rollerball-pen drawing application to form uniform and smooth electrode patterns on cellulose-based paper and polymer-based plastic substrates. The drawn AgNW-GO-Ink conductive lines on paper can achieve conductivity as high as $2.3 \times 10^4 \text{ S cm}^{-1}$ and sheet resistance as low as $0.44 \Omega \text{ sq}^{-1}$

upon drying for only \approx 5 min at 25 °C. Moreover, the introduction of GO makes the AgNW-GO-Ink electrodes exhibit an excellent resistance to the surface oxidation of AgNW during a long-time stability test in hot air. The AgNW-GO-Ink conductive lines drawn on paper can be repeatedly folded with a permanent inelastic crease on the folding line of paper without suffering large degradation on conductivity. The mechanism behind the outstanding foldability of AgNW-GO-Ink electrodes on paper was also explored by microscopy and mechanical model analysis. The AgNW-GO-Ink can be used as foldable electrodes to demonstrate rollerball-pen drawable and foldable paper-based electronic circuits and capacitive touch screen sensors. These results present a promising drawable technology to realize extremely foldable paper-based electronics.

4. Experimental Section

Raw Materials: AgNWs (1 wt% in water) were purchased from Zhejiang Kechuang Advanced Materials Co., Ltd. The average diameter and length of the AgNWs were 25–35 nm and 15–25 μ m. GO with average lateral size around 1 μ m and thickness of \approx 0.8 nm was prepared from graphite by the modified Hummers method.^[46] Fluorosurfactant FC4430 was purchased from 3M. HPMC (average $M_n \approx$ 10 000), PVP ($M_w =$ 24 000) and NaHCO₃ was obtained from Aladdin. Conductive pen with ink based on silver nanoparticles (AgNP-Ink) was obtained from Electroninks Incorporated (Circuit Scribe), and conductive pen with ink using silver microflakes as conductive additives (AgMF-Ink) was supplied by Circuit Works (CW2200). The paper substrates (thickness \approx 88 μ m) were cellulose fiber-based multipurpose printing paper purchased from Deli Group Co., LTD.

Preparation of AgNW-GO-Ink: First, 2 mg mL⁻¹ GO dispersion was made by dispersing GO in distilled water via sonication for 30 min, followed by adjusting the pH value to 6.5 via adding 1 M NaHCO₃ aqueous solution. GO solution was then added into the as-received AgNWs solution with GO to AgNWs weight ratio of 2.5:20, and coagulation appeared immediately. After sonication for about 5 min, the AgNW and GO mixture was vacuum filtration using PTFE membrane filter with pore size of 0.45 μ m, followed by washing with 100 mL distilled water for five times. The collected AgNW-GO precipitate on the membrane filter was redispersed in distilled water with additives of PVP and FC4430 through strong agitation using VORTEX mixer at 1000 rpm for 2 h to obtain the final homogeneous AgNW-GO-Ink. Careful optimization of the mass ratio between AgNW:GO:PVP:FC4430:water and 20:2.5:2:0.2:400 results in simultaneously best attributes of rheological properties, conductivity, stability, and foldability. A very small amount of particulates would appear in the ink after kept still for about one month. A few seconds of mild sonication or a few minutes of agitation using VORTEX mixer at 1000 rpm can redisperse the particulates.

Preparation of AgNW-HPMC-Ink and AgNW-PVP-Ink: To prepare AgNW-HPMC-Ink, HPMC, PVP, and FC4430 were mixed at the weight ratio of 20:20:2:0.2 using VORTEX mixer at 1000 rpm for 1 h, followed by drying the dispersion completely via vacuum rotary evaporation. Then, distilled water was added back to the mixture with the mass ratio between AgNW:HPMC:PVP:FC4430:water and 20:20:2:0.2:400, followed by strong agitation using VORTEX mixer at 1000 rpm for 2 h. A large amount of aggregation was still observed in the AgNW-HPMC-Ink. To prepare AgNW-PVP-Ink, AgNW, PVP, and FC4430 were mixed at the weight ratio of 20:20:0.2 using VORTEX mixer at 1000 rpm for 1 h, followed by drying the dispersion completely via vacuum rotary evaporation. Then, distilled water was added back to the mixture with the mass ratio between AgNW:HPMC:PVP:FC4430:water and 20:20:0.2:400, followed by strong agitation using VORTEX mixer at 1000 rpm for 2 h. A homogeneous dispersion of AgNW-PVP-Ink could be obtained.

Rollerball-Pen Drawing: To fill rollerball pen with our conductive inks, AgNW-GO-Ink or AgNW-PVP-Ink was filled into a new ink barrel from one end of the barrel using a disposable pipette, and the plastic pen tip was assembled. The ink was then forced to the rollerball tip

via air compression on the other end of the pen barrel. All electrodes, conductive traces, and circuits were drawn on papers directly by hand, and patterns of straight lines were drawn with the assist of a ruler. To connect LED chips on the conductive circuits, two terminals of the LED chips were attached on the drawn electrodes with silver paste. All conductive traces were drawn for only one time.

Fabrication of Capacitive Paper-Based Touch Screen System: First, paper-based touch sensor with 8×8 independently controlled sensor pixels was fabricated by drawn row electrodes and column electrodes, both made of eight alternating active electrodes and a ground electrode, respective on the top and bottom side of one piece of paper with a stacked angle of 90°. The width of the active row electrode and the neighboring ground electrode were about 1.5 and 0.5 mm respectively; the width of the active column electrode and the neighboring ground electrode were about 0.75 and 0.5 mm respectively. Next, the paper-based touch sensor was connected to an 8×8 LED display through an Arduino-based touch screen control system to construct an entire capacitive touch screen system. Each LED light was controlled by the corresponding sensor pixel on the paper-based touch sensor. The active row electrodes with width about 1.5 mm were drawn for two times to ensure to achieve the large line width.

Characterization: In order to perform cyclic folding tests, eight parallel conductive lines with dimensions of 20 mm in length and \approx 700–900 μ m in width were first drawn on paper substrates. To ensure the same testing conditions, all electrodes were dried at 80 °C for 30 min before the mechanical test. Testing samples were folded with permanent creases at the point of the folded electrodes and compressed firmly to achieve the smallest possible bending radius when folded by hand (<40 μ m). A Keithley 2000 digital multimeter was used to monitor the resistance change. The thickness of the drawn electrodes was measured by a Dektak profilometer. Rheological behavior of the formulated inks was probed using a DHR-2 rheometer (TA Instruments) with a 25 mm plate system and 800 μ m gap. All measurements were probed at room temperature (\approx 25 °C). A preconditioning step at a shear rate of 0.1 s⁻¹ for 15 s was applied before each test. The steady-state flow step test was performed to measure the shear viscosity of the inks at shear rates of 0.1–1000 s⁻¹, and the PHS test was performed with constant shear rates in three intervals (0.1 s⁻¹ shear rate for 30 s, 100 s⁻¹ for 30 s, and 0.1 s⁻¹ for 100 s) to simulate the rollerball-pen drawing process. The SSS test was performed with oscillation stress of 1–10 Pa at a frequency of 1 Hz.

Supporting Information

Supporting Information is available from the Wiley Online Library or from the author.

Acknowledgements

S.L. and J.L. contributed equally to this work. The work reported here was supported by MoST (2016YFA0200200) and National Natural Science Foundation of China (NSFC51673099 and 51633002).

Conflict of Interest

The authors declare no conflict of interest.

Keywords

drawable conductive ink, foldable paper electronics, graphene oxide, rollerball-pen-drawing technology, silver nanowires

Received: March 10, 2017

Revised: April 6, 2017

Published online: May 16, 2017

- [1] R. H. Kim, H. J. Kim, I. Bae, S. K. Hwang, D. B. Velusamy, S. M. Cho, K. Takaishi, T. Muto, D. Hashizume, M. Uchiyama, P. André, F. Mathevet, B. Heinrich, T. Aoyama, D.-E. Kim, H. Lee, J.-C. Ribierre, C. Park, *Nat. Commun.* **2014**, *5*, 3583.
- [2] W. J. Hyun, E. B. Secor, G. A. Rojas, M. C. Hersam, L. F. Francis, C. D. Frisbie, *Adv. Mater.* **2015**, *27*, 7058.
- [3] W. J. Hyun, O. O. Park, B. D. Chin, *Adv. Mater.* **2013**, *25*, 4729.
- [4] M. J. Han, D. Y. Khang, *Adv. Mater.* **2015**, *27*, 4969.
- [5] R. Z. Li, A. Hu, T. Zhang, K. D. Oakes, *ACS Appl. Mater. Interfaces* **2014**, *6*, 21721.
- [6] A. C. Siegel, S. T. Phillips, M. D. Dickey, N. Lu, Z. Suo, G. M. Whitesides, *Adv. Funct. Mater.* **2010**, *20*, 28.
- [7] G.-W. Huang, H.-M. Xiao, S.-Y. Fu, *Nanoscale* **2014**, *6*, 8495.
- [8] M. M. Hamed, A. Ainla, F. Güder, D. C. Christodouleas, M. T. Fernández-Abedul, G. M. Whitesides, *Adv. Mater.* **2016**, *28*, 5054.
- [9] M. S. White, M. Kaltenbrunner, E. D. Głowacki, K. Gutnichenko, G. Kettlgruber, I. Graz, S. Aazou, C. Ulbricht, D. A. M. Egbe, M. C. Miron, Z. Major, M. C. Scharber, T. Sekitani, T. Someya, S. Bauer, N. S. Sariciftci, *Nat. Photonics* **2013**, *7*, 811.
- [10] M. Kaltenbrunner, T. Sekitani, J. Reeder, T. Yokota, K. Kuribara, T. Tokuhara, M. Drack, R. Schwödiauer, I. Graz, S. Bauer-Gogonea, S. Bauer, T. Someya, *Nature* **2013**, *499*, 458.
- [11] T. Sekitani, U. Zschieschang, H. Klauk, T. Someya, *Nat. Mater.* **2010**, *9*, 1015.
- [12] K. Fukuda, Y. Takeda, Y. Yoshimura, R. Shiwaku, L. T. Tran, T. Sekine, M. Mizukami, D. Kumaki, S. Tokito, *Nat. Commun.* **2014**, *5*, 4147.
- [13] G. A. Salvatore, N. Münzenrieder, T. Kinkeldei, L. Petti, C. Zyss, I. Strelbel, L. Büthe, G. Tröster, *Nat. Commun.* **2014**, *5*, 2982.
- [14] A. Russo, B. Y. Ahn, J. J. Adams, E. B. Duoss, J. T. Bernhard, J. A. Lewis, *Adv. Mater.* **2011**, *23*, 3426.
- [15] N. N. Jason, W. Shen, W. Cheng, *ACS Appl. Mater. Interfaces* **2015**, *7*, 16760.
- [16] Y.-L. Tai, Z.-G. Yang, *J. Mater. Chem.* **2011**, *21*, 5938.
- [17] E. O. Polat, H. B. Uzlu, O. Balci, N. Kakenov, E. Kovalska, C. Kocabas, *ACS Photonics* **2016**, *3*, 964.
- [18] D. J. Finn, M. Lotya, J. N. Coleman, *ACS Appl. Mater. Interfaces* **2015**, *7*, 9254.
- [19] L. Setti, A. Fraleoni-Morgera, B. Ballarin, A. Filippini, D. Frascaro, C. Piana, *Biosens. Bioelectron.* **2005**, *20*, 2019.
- [20] J. Lessing, A. C. Glavan, S. B. Walker, C. Keplinger, J. A. Lewis, G. M. Whitesides, *Adv. Mater.* **2014**, *26*, 4677.
- [21] L. Huang, Y. Huang, J. Liang, X. Wan, Y. Chen, *Nano Res.* **2011**, *4*, 675.
- [22] W.-J. Guan, Y. Li, Y.-Q. Chen, X.-B. Zhang, G.-Q. Hu, *Biosens. Bioelectron.* **2005**, *21*, 508.
- [23] Z. Nie, C. A. Nijhuis, J. Gong, X. Chen, A. Kumachev, A. W. Martinez, M. Narovlyansky, G. M. Whitesides, *Lab Chip* **2010**, *10*, 477.
- [24] D. Tobjörk, R. Österbacka, *Adv. Mater.* **2011**, *23*, 1935.
- [25] J. Y. Kim, S. H. Park, T. Jeong, M. J. Bae, S. Song, J. Lee, I. T. Han, D. Jung, S. Yu, *IEEE Trans. Electron Devices* **2010**, *57*, 1470.
- [26] R. Narayan, J. E. Kim, J. Y. Kim, K. E. Lee, S. O. Kim, *Adv. Mater.* **2016**, *28*, 3045.
- [27] D. R. Dreyer, S. Park, C. W. Bielawski, R. S. Ruoff, *Chem. Soc. Rev.* **2010**, *39*, 228.
- [28] J. Kim, L. J. Cote, J. X. Huang, *Acc. Chem. Res.* **2012**, *45*, 1356.
- [29] C. Vallés, R. J. Young, D. J. Lomax, I. A. Kinloch, *J. Mater. Sci.* **2014**, *49*, 6311.
- [30] S. Nafcy, R. Jalili, S. H. Aboutalebi, R. A. Gorkin Iii, K. Konstantinov, P. C. Innis, G. M. Spinks, P. Poulin, G. G. Wallace, *Mater. Horiz.* **2014**, *1*, 326.
- [31] S. P. Obukhov, *Phys. Rev. Lett.* **1995**, *74*, 4472.
- [32] M. B. Bryning, M. F. Islam, J. M. Kikkawa, A. G. Yodh, *Adv. Mater.* **2005**, *17*, 1186.
- [33] L. J. Cote, J. Kim, V. C. Tung, J. Luo, F. Kim, J. Huang, *Pure Appl. Chem.* **2010**, *83*, 95.
- [34] J. Liang, L. Li, K. Tong, Z. Ren, W. Hu, X. Niu, Y. Chen, Q. Pei, *ACS Nano* **2014**, *8*, 1590.
- [35] J. Liang, K. Tong, Q. Pei, *Adv. Mater.* **2016**, *28*, 5986.
- [36] R. Rudež, J. Pavlič, S. Bernik, *J. Eur. Ceram. Soc.* **2015**, *35*, 3013.
- [37] R. Durairaj, S. Ramesh, S. Mallik, A. Seman, N. Ekere, *Mater. Des.* **2009**, *30*, 3812.
- [38] R. Faddoul, N. Reverdy-Bruas, J. Bourel, *J. Mater. Sci.: Mater. Electron.* **2012**, *23*, 1415.
- [39] R. Durairaj, S. Mallik, A. Seman, A. Marks, N. N. Ekere, *J. Mater. Processes Technol.* **2009**, *209*, 3923.
- [40] I. K. Moon, J. I. Kim, H. Lee, K. Hur, W. C. Kim, H. Lee, *Sci. Rep.* **2013**, *3*, 1.
- [41] M.-S. Lee, K. Lee, S.-Y. Kim, H. Lee, J. Park, K.-H. Choi, H.-K. Kim, D.-G. Kim, D.-Y. Lee, S. Nam, J.-U. Park, *Nano Lett.* **2013**, *13*, 2814.
- [42] N. H. De Leeuw, C. J. Nelson, *J. Phys. Chem. B* **2003**, *107*, 3528.
- [43] I. Lončarić, V. Despoja, *Phys. Rev. B: Condens. Matter Mater. Phys.* **2014**, *90*, 1.
- [44] J. Li, J. J. Liang, L. Li, F. Ren, W. Hu, J. Li, S. Qi, Q. Pei, *ACS Nano* **2014**, *8*, 12874.
- [45] Capacitance Meter and RC Time Constants, <http://arduino.cc/en/Tutorial/CapacitanceMeter> (accessed December 2016).
- [46] D. A. Dikin, S. Stankovich, E. J. Zimney, R. D. Piner, G. H. B. Domke, G. Evmenenko, S. T. Nguyen, R. S. Ruoff, *Nature* **2007**, *448*, 457.

Copyright WILEY-VCH Verlag GmbH & Co. KGaA, 69469 Weinheim, Germany, 2017.



Supporting Information

for *Adv. Electron. Mater.*, DOI: 10.1002/aelm.201700098

Rollerball-Pen-Drawing Technology for Extremely Foldable Paper-Based Electronics

Shuiren Liu, Junpeng Li, Xinlei Shi, Enlai Gao, Zhiping Xu, Honghao Tang, Kwing Tong, Qibing Pei, Jiajie Liang, and Yongsheng Chen*

Supporting Information

DOI: 10.1002/aelm.201700098

Rollerball-Pen-Drawing Technology for Extremely Foldable Paper-Based Electronics

By *Shuiren Liu⁺, Junpeng Li⁺, Xinlei Shi, Enlai Gao, Zhiping Xu, Honghao Tang, Kwing Tong, Qibing Pei, Jiajie Liang**, and *Yongsheng Chen*

[*] Prof. J. Liang, Mr. S. Liu, Mr. X. Shi, Mr. H. Tang, Prof. Y. Chen

School of Materials Science and Engineering

National Institute for Advanced Materials

Nankai University

Tianjin 300350, China

E-mail: liang0909@nankai.edu.cn

Prof. J. Liang, Prof. Y. Chen

Key Laboratory of Functional Polymer Materials of Ministry of Education

College of Chemistry

Nankai University

Tianjin 300350, China

Dr. J. Li

School of Science

Xi'an University of Technology

Xi'an, Shaanxi 710048, China

Mr. E. Gao, Prof. Z. Xu

Applied Mechanics Laboratory

Department of Engineering Mechanics and Center for Nano and Micro Mechanics

Tsinghua University

Beijing 100084, China

Mr. K. Tong, Prof. Q. Pei

Department of Materials Science and Engineering

Henry Samueli School of Engineering and Applied Science

University of California, Los Angeles

Los Angeles, CA 90095, USA



Figure S1. Photograph of the as-prepared AgNW-HPMC-Ink showing obvious aggregations of the AgNWs on the sidewalls of the container.

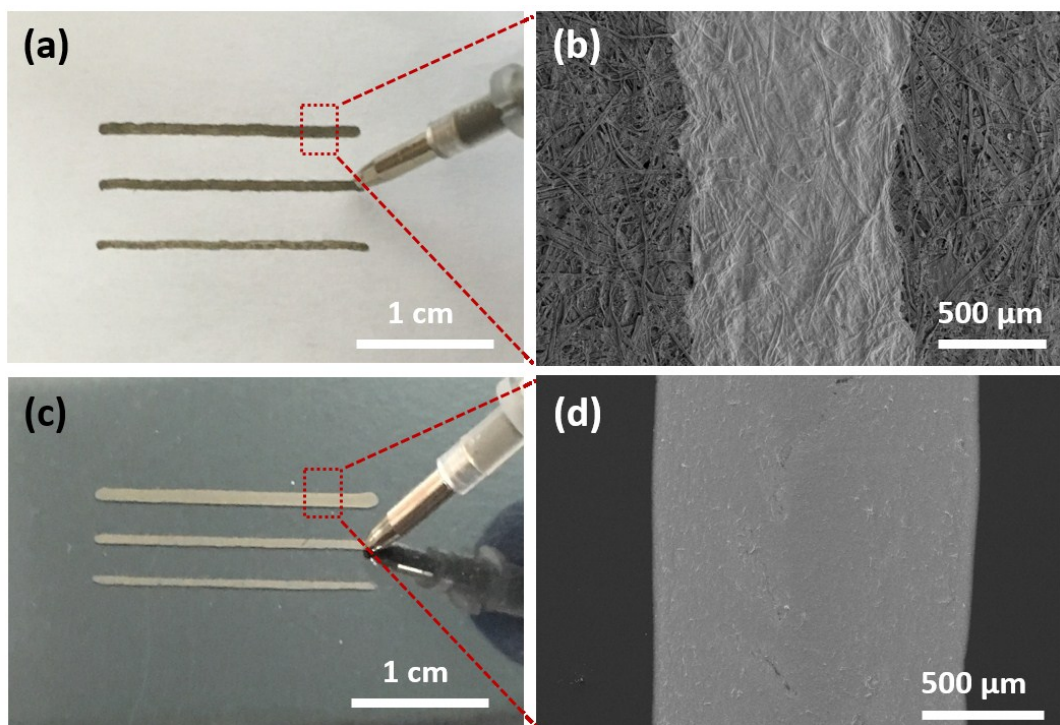


Figure S2. Optical image of AgNW-GO-Ink electrodes with different width drawn on (a) a paper and (c) a PET substrate by rollerball pen with different ball diameters. SEM image of the top view of a AgNW-GO-Ink electrode on (b) a paper and (d) a PET substrate drawn by rollerball pen with ball diameter of 960 μm . Compared to the traces drawn on paper, the AgNW-GO-Ink traces drawn on PET film exhibited a larger line width (~ 1,100 with a ball diameter of 960 μm as shown in Figure S2), which was attributed to the feature of water absorption of the cellulose fibers in the paper substrate and thus can limit the ink spreading during rollerball-pen drawing.

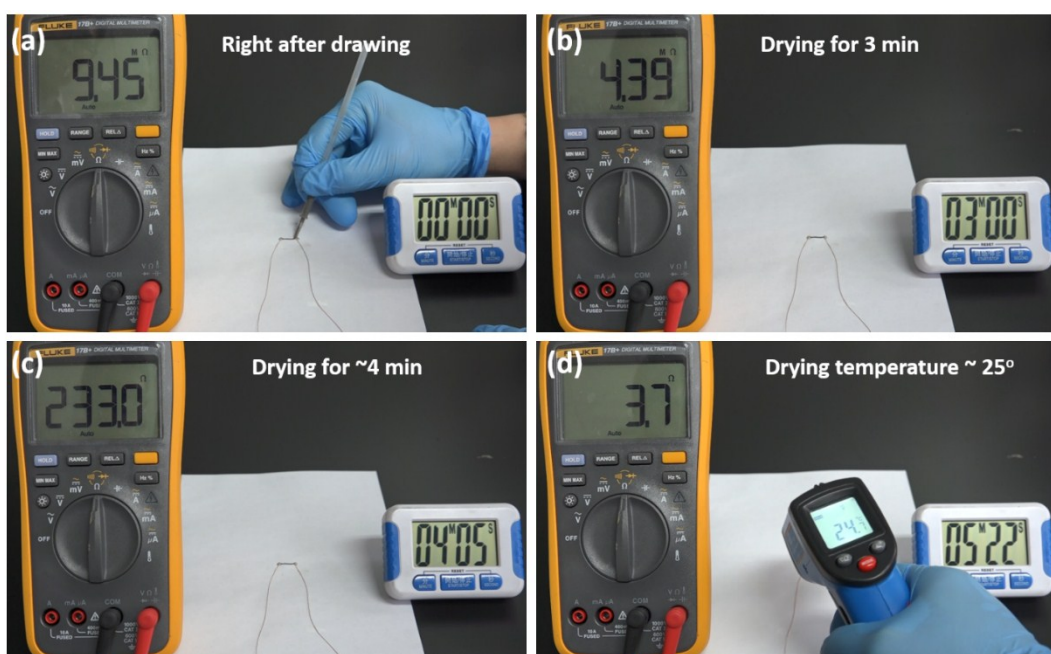


Figure S3. The resistance change during the whole post-treatment process of drying at 25° for the AgNW-GO-Ink electrode right after drawn on paper.

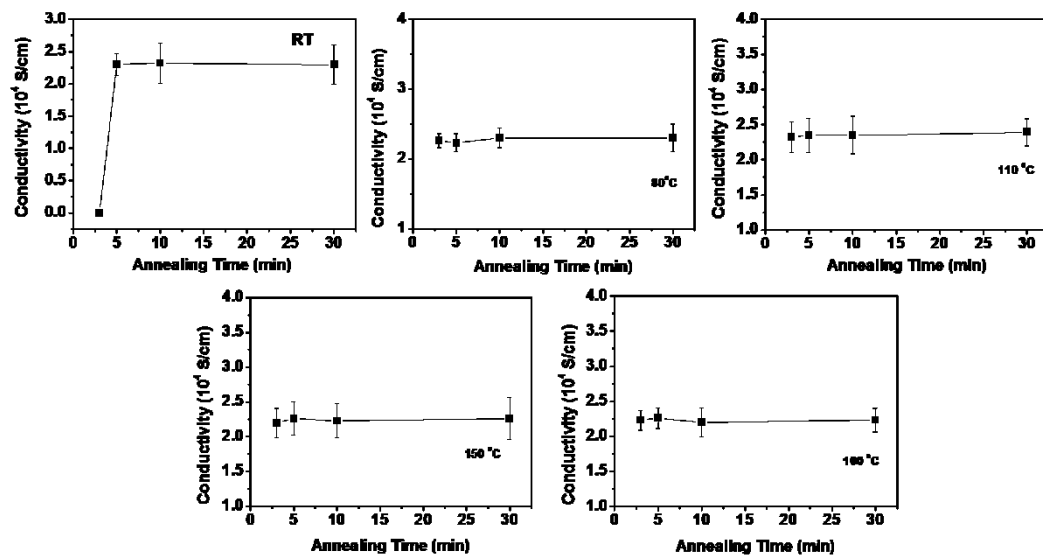


Figure S4. Average electrical conductivity of AgNW-GO-Ink electrodes with standard deviations as a function of drying temperature and time. More than five samples were measured.

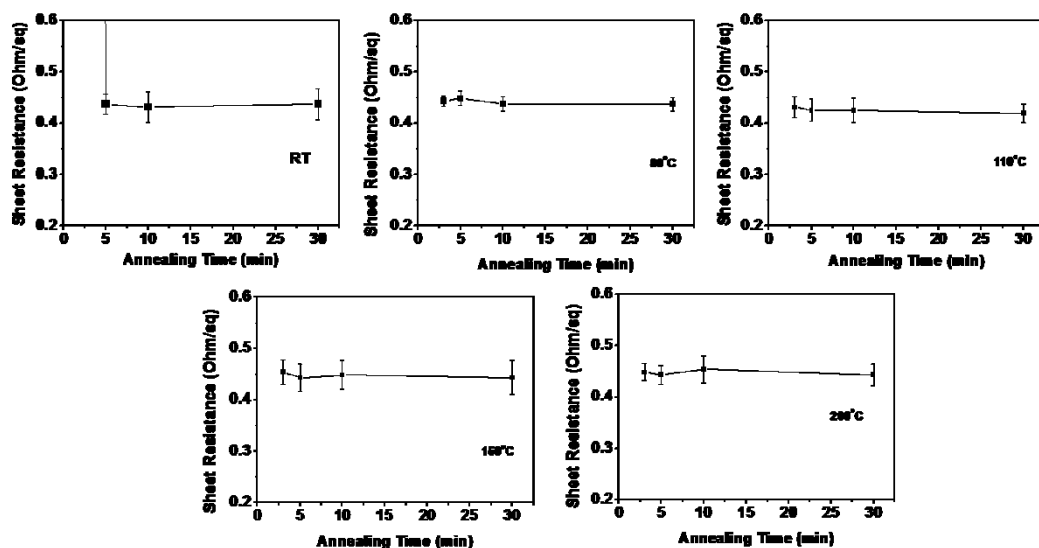


Figure S5. Average sheet resistance of AgNW-GO-Ink electrodes with standard deviations as a function of drying temperature and time. More than five samples were measured.

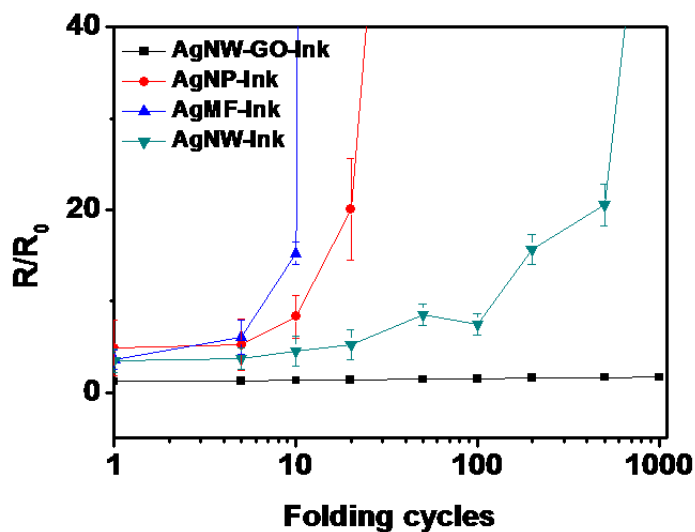


Figure S6. Plots of relative resistance change with standard deviations *versus* time for AgNW-GO-Ink, AgNW-PVP-Ink, AgNP-Ink and AgMF-Ink electrodes drawn on paper substrates after exposure to hot air at 60 °C for 30 days. More than five samples for each electrodes were measured.

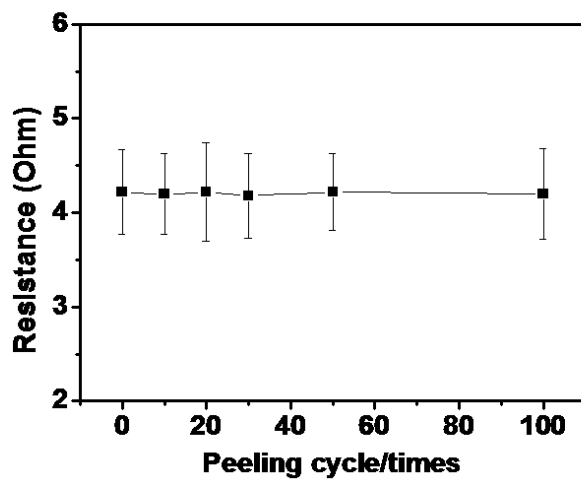


Figure S7. Resistance changes of AgNW-GO-Ink drawn on PET substrate with 100 cycles of adhesion and peeling with Scotch® tape.

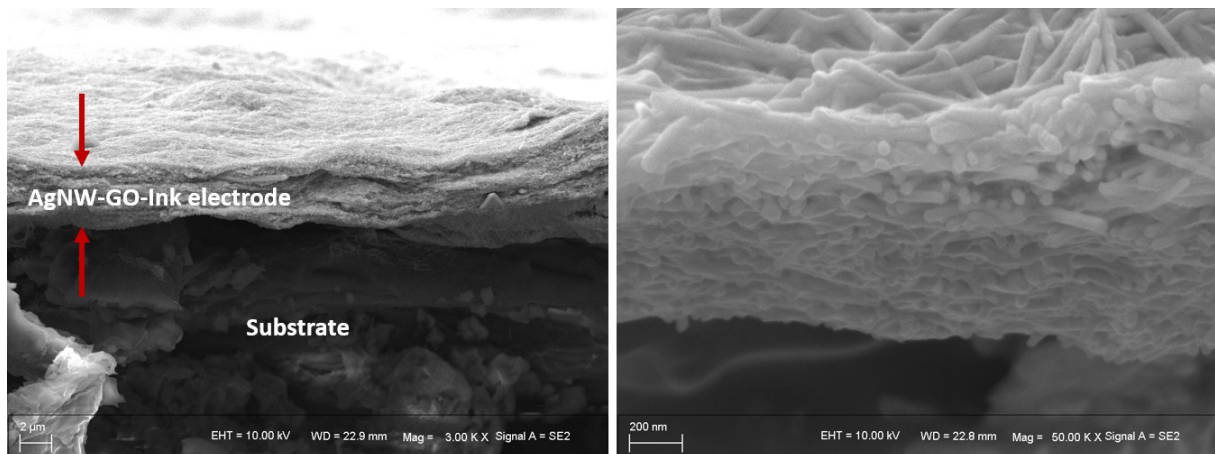


Figure S8. The cross-sectional SEM images of AgNW-GO-Ink electrode drawn on paper substrate.

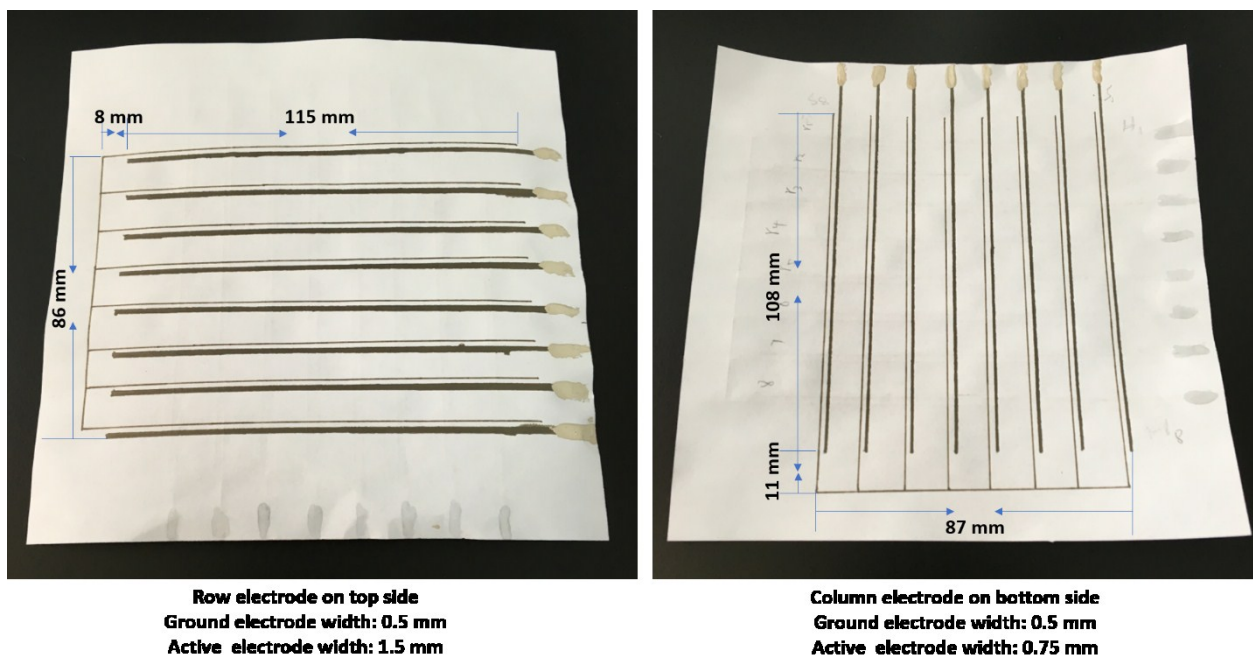


Figure S9. The dimension of the touch sensor with row electrodes on top side and column electrodes on bottom side. The width of active electrode and the neighboring ground electrode is 1.5 mm and 0.5 mm respectively for row electrodes; the width of active electrode and the neighboring ground electrode is 0.75 mm and 0.5 mm respectively for column electrodes.

The paper-based capacitive touch sensor with an array of 8×8 capacitive touch sensing points was then connected to an 8×8 LED display through an Arduino-based touch screen control system to construct an entire capacitive touch screen system.

Response time, defined as the elapsed time to charge the system capacitor in the RC circuitry, can be expressed as:

$$t = RC \ln [V_u / (V_u - V_t)] \quad (1)$$

where V_u and V_t are the input potential and the potential on the capacitor at time t , respectively. C represent the capacitance along the circuitry. Arduino is a microcontroller capable of applying 5 V as a step input to a resistor and a capacitor in series and measuring the time required for the potential on the capacitor to reach 2 V. When reaching 2 V in response to a step input of 5 V, the response time has the following relationship with RC :

$$t = RC \ln(5/3)$$

To adjust sensitivity and stability, an extra resistor (R_e) of 5 k Ω is placed in series with the coupling electrodes. Resistance (R) for a couple of electrodes should be:

$R = R_a + R_b + R_e$, R_a , R_b represent the resistance active electrode and the neighboring ground electrode, respectively. The capacitance along the circuitry could be detected through capacitance meter and the Response time could be obtained.

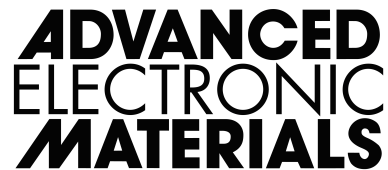
Supplementary Movies:

Supplementary Movie S1: The conductivity of AgNW-GO-Ink electrode can be recovered right after drawn on paper for drying at 25 °C in ~ 5 min.

Supplementary Movie S2: LED chips with AgNW-GO-Ink circuits drawn on paper substrates under cyclic folding-unfolding operated by hand.

Supplementary Movie S3: Demonstration of the foldable paper-based touch screen system.

Copyright WILEY-VCH Verlag GmbH & Co. KGaA, 69469 Weinheim, Germany, 2017.



Supporting Information

for *Adv. Electron. Mater.*, DOI: 10.1002/aelm.201700098

Rollerball-Pen-Drawing Technology for Extremely Foldable Paper-Based Electronics

Shuiren Liu, Junpeng Li, Xinlei Shi, Enlai Gao, Zhiping Xu, Honghao Tang, Kwing Tong, Qibing Pei, Jiajie Liang, and Yongsheng Chen*

Supporting Information

DOI: 10.1002/aelm.201700098

Rollerball-Pen-Drawing Technology for Extremely Foldable Paper-Based Electronics

By *Shuiren Liu⁺, Junpeng Li⁺, Xinlei Shi, Enlai Gao, Zhiping Xu, Honghao Tang, Kwing Tong, Qibing Pei, Jiajie Liang**, and *Yongsheng Chen*

[*] Prof. J. Liang, Mr. S. Liu, Mr. X. Shi, Mr. H. Tang, Prof. Y. Chen

School of Materials Science and Engineering

National Institute for Advanced Materials

Nankai University

Tianjin 300350, China

E-mail: liang0909@nankai.edu.cn

Prof. J. Liang, Prof. Y. Chen

Key Laboratory of Functional Polymer Materials of Ministry of Education

College of Chemistry

Nankai University

Tianjin 300350, China

Dr. J. Li

School of Science

Xi'an University of Technology

Xi'an, Shaanxi 710048, China

Mr. E. Gao, Prof. Z. Xu

Applied Mechanics Laboratory

Department of Engineering Mechanics and Center for Nano and Micro Mechanics

Tsinghua University

Beijing 100084, China

Mr. K. Tong, Prof. Q. Pei

Department of Materials Science and Engineering

Henry Samueli School of Engineering and Applied Science

University of California, Los Angeles

Los Angeles, CA 90095, USA



Figure S1. Photograph of the as-prepared AgNW-HPMC-Ink showing obvious aggregations of the AgNWs on the sidewalls of the container.

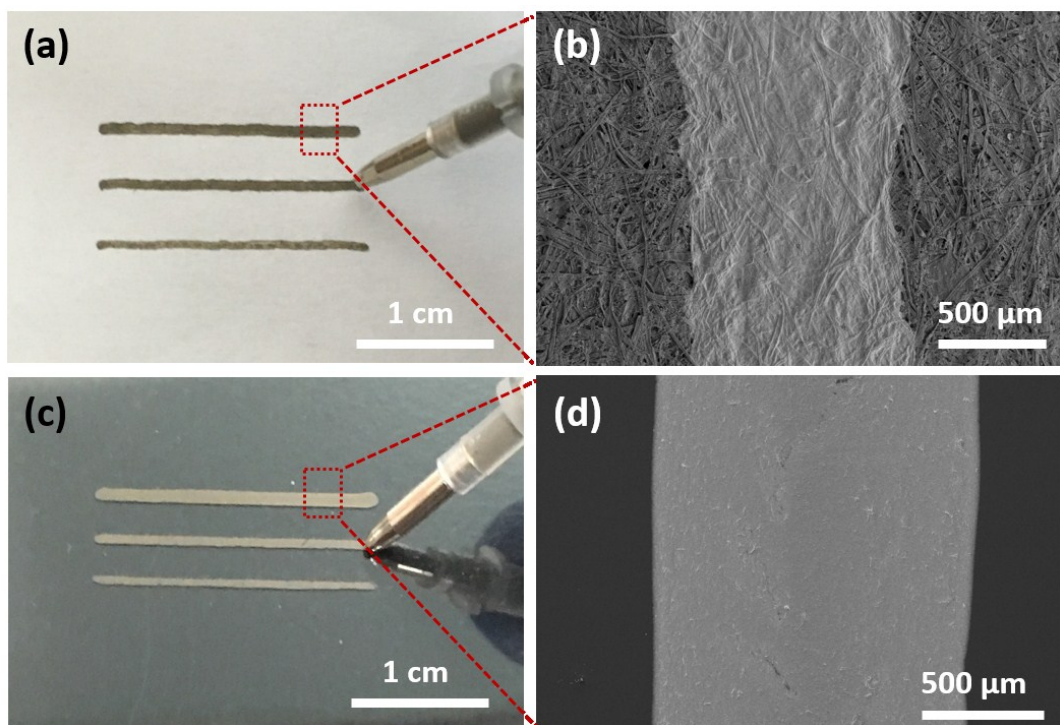


Figure S2. Optical image of AgNW-GO-Ink electrodes with different width drawn on (a) a paper and (c) a PET substrate by rollerball pen with different ball diameters. SEM image of the top view of a AgNW-GO-Ink electrode on (b) a paper and (d) a PET substrate drawn by rollerball pen with ball diameter of 960 μm . Compared to the traces drawn on paper, the AgNW-GO-Ink traces drawn on PET film exhibited a larger line width (~ 1,100 with a ball diameter of 960 μm as shown in Figure S2), which was attributed to the feature of water absorption of the cellulose fibers in the paper substrate and thus can limit the ink spreading during rollerball-pen drawing.

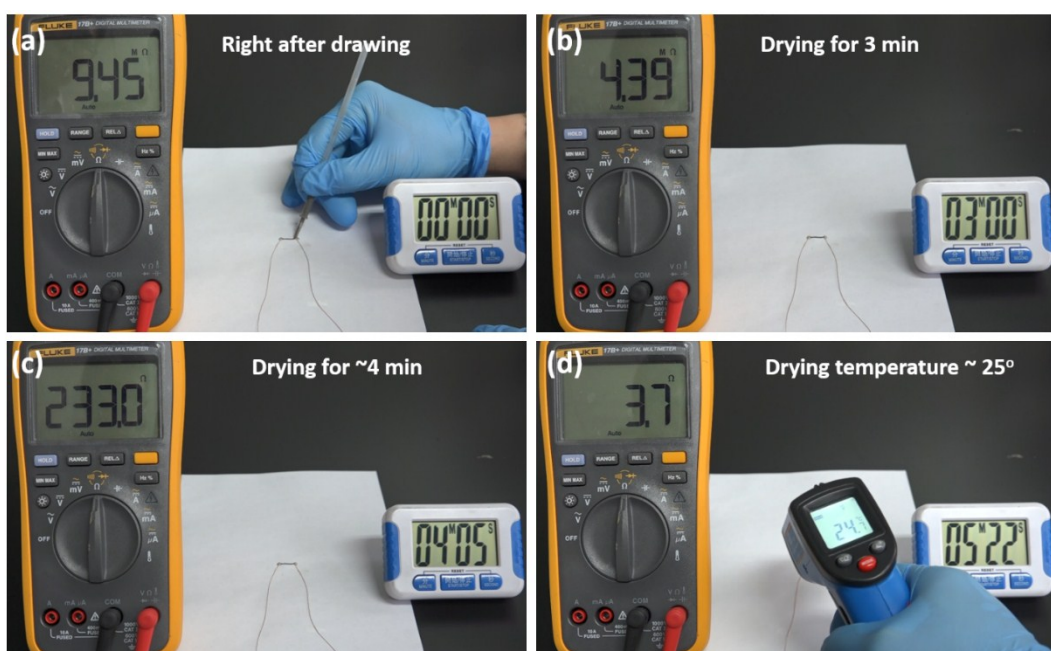


Figure S3. The resistance change during the whole post-treatment process of drying at 25° for the AgNW-GO-Ink electrode right after drawn on paper.

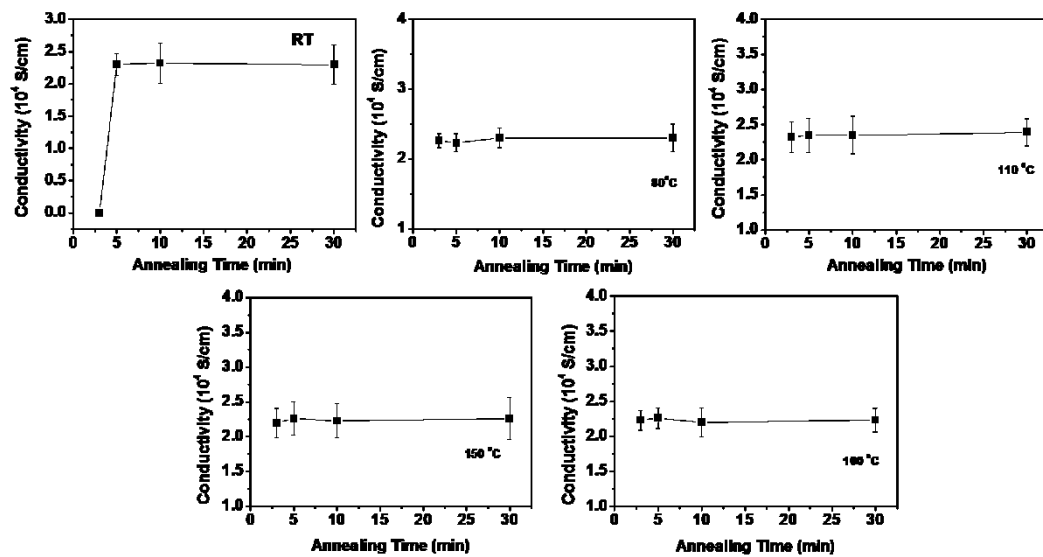


Figure S4. Average electrical conductivity of AgNW-GO-Ink electrodes with standard deviations as a function of drying temperature and time. More than five samples were measured.

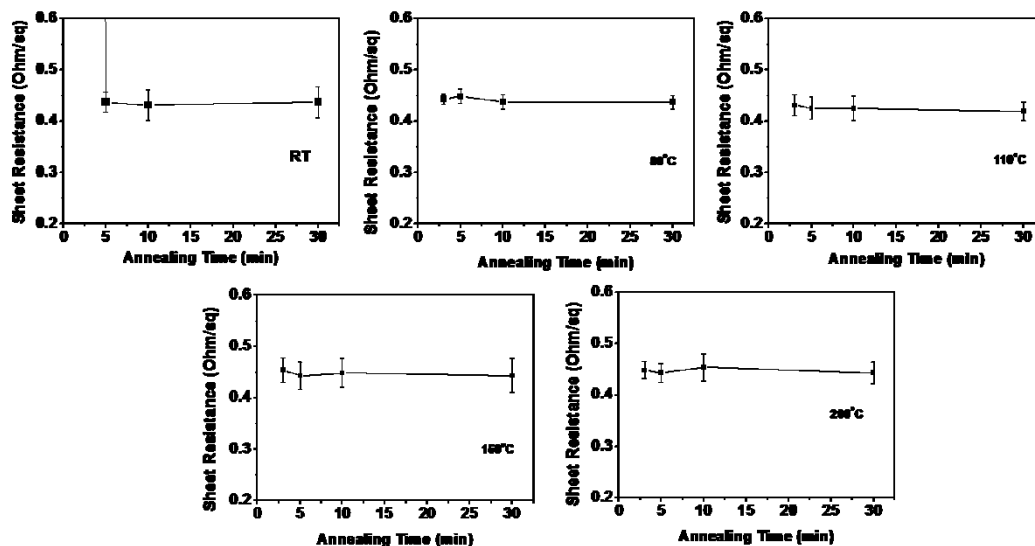


Figure S5. Average sheet resistance of AgNW-GO-Ink electrodes with standard deviations as a function of drying temperature and time. More than five samples were measured.

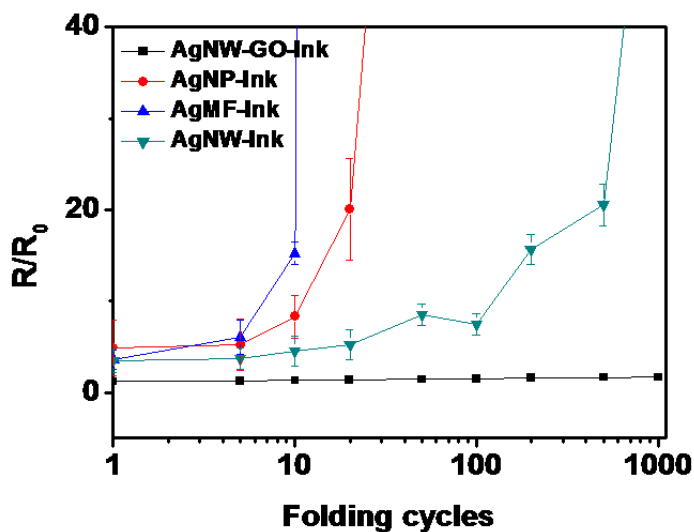


Figure S6. Plots of relative resistance change with standard deviations *versus* time for AgNW-GO-Ink, AgNW-PVP-Ink, AgNP-Ink and AgMF-Ink electrodes drawn on paper substrates after exposure to hot air at 60 °C for 30 days. More than five samples for each electrodes were measured.

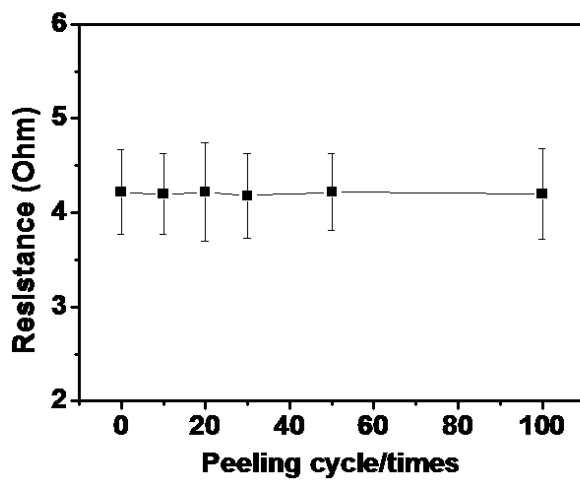


Figure S7. Resistance changes of AgNW-GO-Ink drawn on PET substrate with 100 cycles of adhesion and peeling with Scotch® tape.

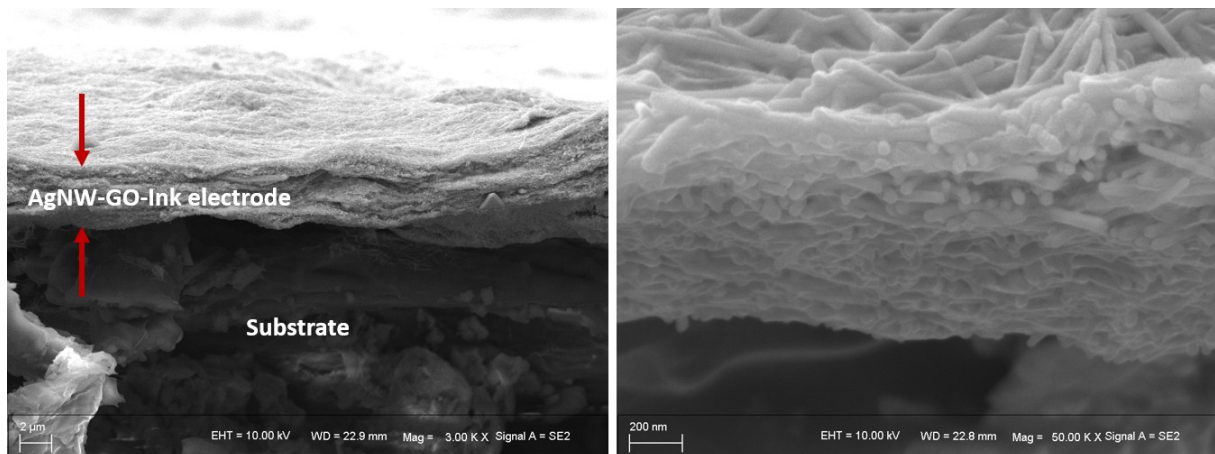


Figure S8. The cross-sectional SEM images of AgNW-GO-Ink electrode drawn on paper substrate.

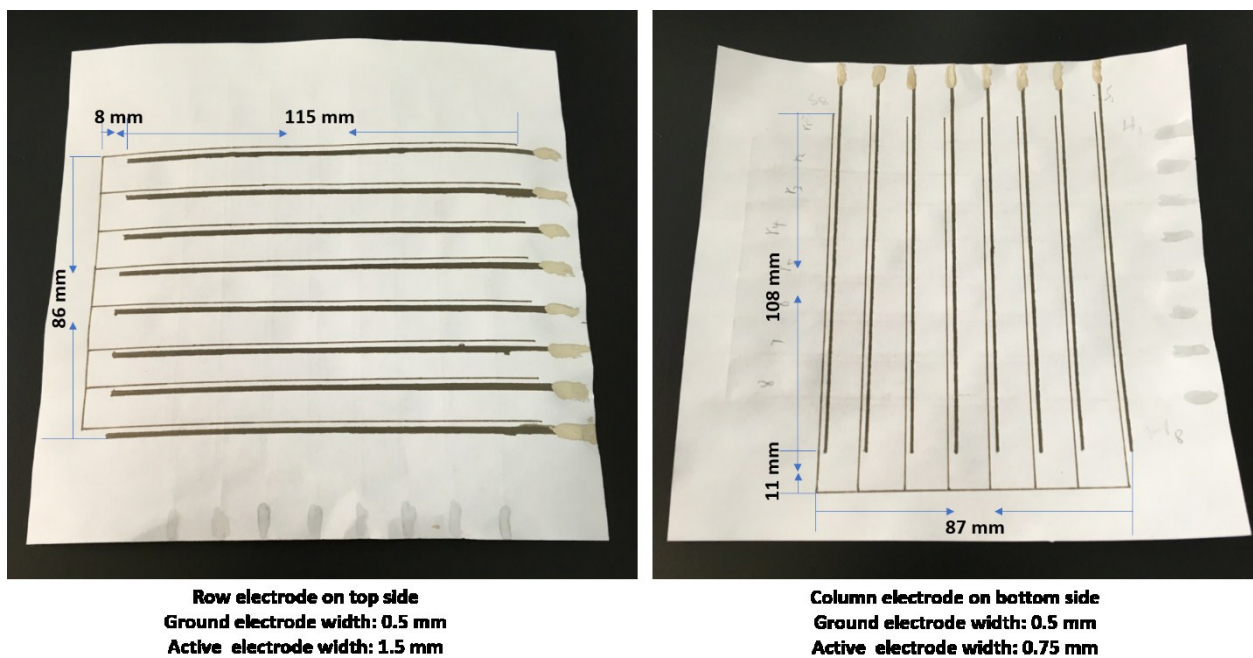


Figure S9. The dimension of the touch sensor with row electrodes on top side and column electrodes on bottom side. The width of active electrode and the neighboring ground electrode is 1.5 mm and 0.5 mm respectively for row electrodes; the width of active electrode and the neighboring ground electrode is 0.75 mm and 0.5 mm respectively for column electrodes.

The paper-based capacitive touch sensor with an array of 8×8 capacitive touch sensing points was then connected to an 8×8 LED display through an Arduino-based touch screen control system to construct an entire capacitive touch screen system.

Response time, defined as the elapsed time to charge the system capacitor in the RC circuitry, can be expressed as:

$$t = RC \ln [V_u / (V_u - V_t)] \quad (1)$$

where V_u and V_t are the input potential and the potential on the capacitor at time t , respectively. C represent the capacitance along the circuitry. Arduino is a microcontroller capable of applying 5 V as a step input to a resistor and a capacitor in series and measuring the time required for the potential on the capacitor to reach 2 V. When reaching 2 V in response to a step input of 5 V, the response time has the following relationship with RC:

$$t = RC \ln(5/3)$$

To adjust sensitivity and stability, an extra resistor (R_e) of 5 k Ω is placed in series with the coupling electrodes. Resistance (R) for a couple of electrodes should be:

$R = R_a + R_b + R_e$, R_a , R_b represent the resistance active electrode and the neighboring ground electrode, respectively. The capacitance along the circuitry could be detected through capacitance meter and the Response time could be obtained.

Supplementary Movies:

Supplementary Movie S1: The conductivity of AgNW-GO-Ink electrode can be recovered right after drawn on paper for drying at 25 °C in ~ 5 min.

Supplementary Movie S2: LED chips with AgNW-GO-Ink circuits drawn on paper substrates under cyclic folding-unfolding operated by hand.

Supplementary Movie S3: Demonstration of the foldable paper-based touch screen system.